Inorganic Chemistry

Article

pubs.acs.org/IC

# Fully Delocalized (Ethynyl)(vinyl)phenylene Bridged Triruthenium Complexes in up to Five Different Oxidation States†

Evelyn Wuttke,‡ Florian Pevny,‡ Yves-Marie Hervault,§ Lucie Norel,§ Malte Drescher,‡ Rainer F. Winter,*,‡ and Stéphane Rigaut*,§

‡Fachbereich Chemie, Universität Konstanz, Universitätsstraße 10, D-78453 Konstanz, Germany

§Sciences Chimiques de Rennes, UMR 6226 CNRS-Université de Rennes 1, Campus de Beaulieu, F-35042, Rennes Cedex, France

Supporting Information

**ABSTRACT:** Triruthenium $[(dppe)_2Ru\{-C{\equiv}C-1,4-C_6H_2-2,5-R_2-CH{=}CH-RuCl(CO)(P^iPr_3)_2\}_2]^{n+}$ (**4a**, R = H; **4b**, R = OMe) containing unsymmetrical (ethynyl)(vinyl)-phenylene bridging ligands and displaying five well-separated redox states ($n$ = 0−4) are compared to their bis(alkynyl) ruthenium precursors $(dppe)_2Ru\{-C{\equiv}C-1,4-C_6H_2-2,5-R_2-C{\equiv}CR'\}$ (**2a**,**b**: R′ = TMS; **3a**,**b**: R′ = H) and their symmetrically substituted bimetallic congeners, complexes $\{Cl(dppe)_2Ru\}_2\{\mu\text{-}C{\equiv}C-1,4-C_6H_2-2,5-R_2-C{\equiv}C\}$ ($\mathbf{A_a}$, R = H; $\mathbf{A_b}$, R = OMe) and $\{RuCl(CO)(P^iPr_3)_2\}_2\{\mu\text{-}CH{=}CH-1,4-C_6H_2-2,5-R_2-CH{=}CH\}$ ($\mathbf{V_a}$, R = H; $\mathbf{V_b}$, R = OMe) as well as the mixed (ethynyl)(vinyl)phenylene bridged $[Cl(dppe)_2Ru-C{\equiv}C-1,4-C_6H_4-CH{=}CH-RuCl(CO)(P^iPr_3)_2]$ ($\mathbf{M_a}$). Successive one-electron transfer steps were studied by means of cyclic voltammetry, EPR and UV−vis−NIR−IR spectroelectrochemistry. These studies show that the first oxidation mainly involves the central bis(alkynyl) ruthenium moiety with only limited effects on the appended vinyl ruthenium moieties. The second to fourth oxidations ($n$ = 2, 3, 4) involve the entire carbon-rich conjugated path of the molecule with an increased charge uniformly distributed between the two arms of the molecules, including the terminal vinyl ruthenium sites. In order to assess the charge distribution, we judiciously use $^{13}CO$ labeled analogues to distinguish stretching vibrations due to the acetylide triple bonds and the intense and charge-sensitive Ru(CO) IR probe in different oxidation states. The comparison between complex pairs $\mathbf{4a,b}^{n+}$ ($n$ = 0−3), $\mathbf{A_{a,b}}^{n+}$ and $\mathbf{V_{a,b}}^{n+}$ ($n$ = 0−2) serves to elucidate the effect of the methoxy donor substituents on the redox and spectroscopic properties of these systems in their various oxidation states and on the metal/ligand contributions to their frontier orbitals.

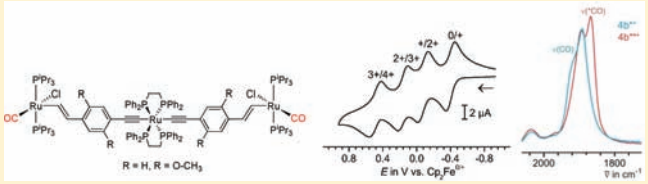


## INTRODUCTION

Oligonuclear ligand-bridged metal complexes displaying ligand-mediated electronic effects have attracted increasing interest.[1−3] In particular, several wirelike transition metal complexes with direct $\sigma$-bond connection of the carbon-rich bridges with the metal atoms have shown excellent abilities to provide a strong electronic interaction between the remote redox-active metal centers,[3] and to achieve electrotriggered functional materials.[4−7] However, a "classical" description of a bridging ligand allowing for electron exchange between the reduced and oxidized termini in mixed-valent states and the general denominations $M^{(n+1)}$ or $M^{(n-1)}$ often used for an oxidized or reduced species are clearly not adequate for ruthenium systems with alkynyl or vinyl ligands. Owing to the substantial ligand character of the highest occupied molecular orbital (HOMO) resulting from the overlap of a metal d$\pi$- and an appropriate $\pi$-orbital of the carbon-rich bridging ligand, the charge density changes at the metal atoms are appreciably lower than would be the case for a metal-centered redox process.

In particular, with ethynyl ruthenium complexes of the type $XRu(dppe)_2(C{\equiv}C-aryl)$ (dppe =1,2-bis(diphenylphosphanyl)ethane, X = anionic ligand)[3a,8−10] or $Cp^RRuL_2(C{\equiv}CR)$[11] and vinyl ruthenium complexes $L(PR_3)_2(CO)Ru(CH{=}CH-aryl)$ (L = neutral two-electron donor ligand or free coordination site),[3f,12] the level of involvement of the carbon-rich ligand in the redox processes is found to be major, with a reduced metal contribution. Those cations can thus be viewed as predominantly organic-centered radicals, the HOMO of the vinylene system receiving even higher contributions from the unsaturated organic ligand, and they are capable of promoting long-range electronic interactions in bimetallic assemblies owing to extensive electron delocalization between the appended metal donor "substituents". The ability of ruthenium to operate as a connector allowing electron flow to occur between different elements in *trans*-ditopic systems,[8,10,13,14] in contrast to other metals such as platinum,[15] was also demonstrated. In particular, with the fragment $[RuCl_n(dppe)_2]$ ($n$ = 0, 1) linear and "W"-shaped molecular wires with three similar metal centers prevent single electron trapping on one part of the structure in different oxidation/reduction states, and display spin density uniformly distributed between the metal atoms and the carbon atoms of the chains.[8,10b,c]

Because potential molecular wires display properties strongly connected to their structure, our current work addresses the issue of long-range electronic interactions in new mixed ethynylvinylarylene-bridged di- and oligonuclear ruthenium complexes relevant to molecule-based hole-conducting materials.[16]

**Received:** October 14, 2011
**Published:** January 6, 2012

   dx.doi.org/10.1021/ic2022177 | *Inorg. Chem.* 2012, 51, 1902−1915

**Chart 1**

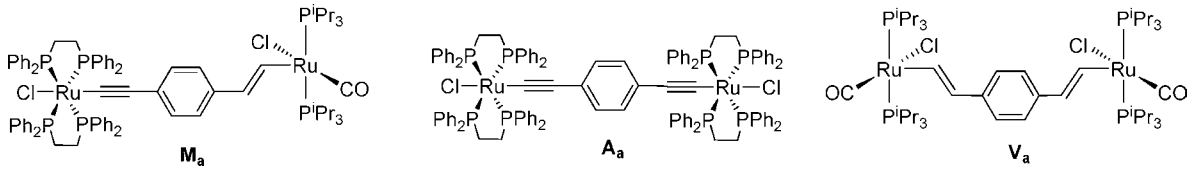


**Scheme 1. Synthetic Pathway for the Trimetallic Adducts 4a,b**

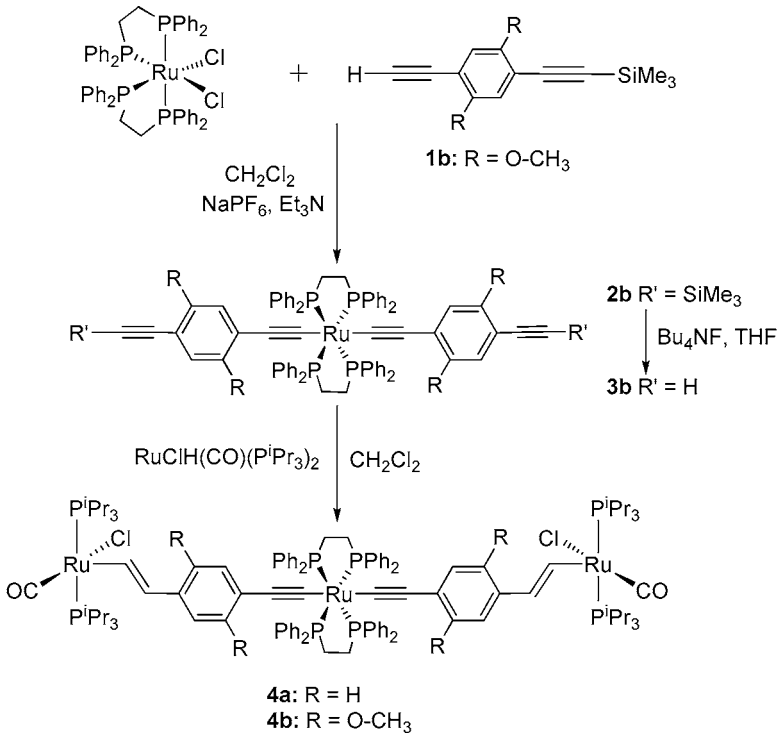


In order to probe for the viability of that concept, we first investigated the mixed ethynyl-vinyl-substituted complex ClRu(dppe)$_2$–C≡C–C$_6$H$_4$–CH=CH–RuCl(CO)(P$^i$Pr$_3$)$_2$ **M$_a$** (Chart 1) and its phenylethynyl substitution product PhC≡C–Ru(dppe)$_2$–C≡C–C$_6$H$_4$–CH=CH–RuCl(CO)(P$^i$Pr$_3$)$_2$ **M$_{ph}$**.[17] We showed that the unsymmetrically bridged complex **M$_a^{\bullet+}$** is a bridge centered radical cation featuring an extended Ru–C≡C–1,4-C$_6$H$_4$–CH=CH–Ru organometallic $\pi$-system with the same charge densities on the Ru–C≡C and Ru–CH=CH termini as they are present in its symmetrical counterparts [ClRu(dppe)$_2$–C≡C–C$_6$H$_4$–C≡C–Ru(dppe)$_2$Cl]$^{\bullet+}$ (**A$_a^{\bullet+}$**)[10a] and [(P$^i$Pr$_3$)$_2$(CO)ClRu–CH=CH–C$_6$H$_4$–CH=CH–RuCl(CO)(P$^i$Pr$_3$)$_2$]$^{\bullet+}$ (**V$_a^{\bullet+}$**).[12e] This suggests that such (ethynyl)(vinyl)phenylene bridging motifs are as efficient as the bis(ethynyl) or bis(vinyl) phenylene ones at effecting charge and spin delocalization over longer distances. As for Ru(dppe)$_2$(–C≡CR)$_2$ *trans*-ditopic systems the SOMO of the oxidized complex extends over *both* alkynyl ligands, it seemed therefore feasible that complexes of higher nuclearity and longer conjugation lengths are capable of communicating electronic information over even longer distances.

We report herein the synthesis and the study of two triruthenium complexes (dppe)$_2$Ru{–C≡C–1,4-C$_6$H$_2$–2,5-R$_2$–CH=CH–RuCl(CO)(P$^i$Pr$_3$)$_2$}$_2$ (**4a**, R = H; **4b**, R = OMe) bearing two 1-ethynyl-4-vinyl phenylene bridges. These compounds were designed with two parameters in mind: (i) to promote electronic interactions over long distances with a larger bridging ligand participation to the redox event than in the pure acetylide systems, and (ii) to modulate the spin density on these bridging ligands upon oxidation with the introduction of electron releasing substituents in their aromatic unit.[9a] Therefore, using a combination of electrochemical and spectroscopic (UV–vis–NIR–IR and EPR) techniques, we illustrate with the studies of different oxidation states the remarkable efficiency of electronic delocalization between the three metal atoms through the two *trans* carbon-rich ligands and the role of the bridging units. To that end, and for a better understanding of the effect of the methoxy groups, we also describe the synthesis and the study of the bimetallic methoxy analogues of **A$_a$** and **V$_a$**, **A$_b$** and **V$_b$**. Also, for the first time with such complexes, we judiciously use $^{13}$CO labeled analogues to disseminate overlapping vibration stretches due to the acetylide triple bonds and to the intense and charge-sensitive Ru(CO) IR probe in different oxidation states. The latter probe appeared to be extremely powerful to provide clear information on the charge distribution over the two arms.

## RESULTS AND DISCUSSION

**Synthesis of the Organometallic Wires.** The trimetallic complexes **4a** and **4b** were achieved by reacting 1 equiv of the bis(alkynyl) complexes (dppe)$_2$Ru(–C≡C–1,4-C$_6$H$_2$–2,5-R$_2$–C≡C–H)$_2$ (**3a**, R = H;[18] **3b**, R = OMe) bearing two activable alkyne functions as a central core, and 2 equiv of the hydride ruthenium complex RuClH(CO)(P$^i$Pr$_3$)$_2$[19] in dichloromethane (Scheme 1). These reactions involve the regio- and


dx.doi.org/10.1021/ic2022177 | Inorg. Chem. 2012, 51, 1902–1915

stereospecific insertion of the terminal alkyne into the Ru−H bond of the hydride complex and provide 1,2-disubstituted vinyl ligands with a *trans* disposition of the metal atom and the aryl substituent on each side in excellent yields (95% and 91%, respectively). The preparation of the new precursor **3b** bearing methoxy groups was achieved with the use of *cis*-$(dppe)_2RuCl_2$ and of the appropriate alkyne **1b**[20] in the presence of a non-coordinating salt ($NaPF_6$) and a base ($Et_3N$) in 92% yield, according to the general procedure previously developed in our laboratory to obtain bis(σ-arylacetylide) complexes,[21,10b,c] and followed by the deprotection of the two alkyne functions with $Bu_4NF$. In addition, the two symmetrical reference complexes $\mathbf{A_b}$ and $\mathbf{V_b}$ were achieved using the same reactions from 1,4-diethynyl-2,5-dimethoxybenzene[22] (Scheme 2). The new

**Scheme 2. Synthetic Pathway for the New Bimetallic References $A_b$ and $V_b$**

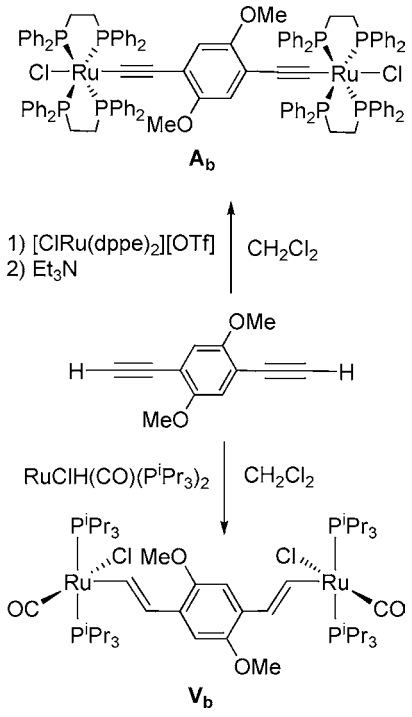


compounds, including the final trimetallic wires, were characterized by means of $^{31}P$, $^{1}H$, $^{13}C$ NMR, and IR spectroscopy and mass spectrometry, as well as with elemental analysis. As an example for **4a**, particularly informative are the two sharp singlets at $\delta$ = 54.1 (dppe) and 39.2 ($P^iPr_3$) ppm in $^{31}P$ NMR spectroscopy. This first signal is characteristic of bis(σ-arylacetylide) species and of the *trans* disposition of two carbon-rich chains on the central ruthenium atom, whereas the second is characteristic of the appended vinyl ruthenium moieties. The presence of both the ruthenium vinyl and ruthenium ethynyl groups also follows from the observation of the typical Ru−C≡*C* and Ru−*C*H=CH resonance signals at $\delta$ = 116.6 (Ru−C≡*C*), 147.9 (Ru−*C*H) and 134.5 (Ru−CH=*C*H) ppm in $^{13}C$ NMR spectroscopy. In the $^{1}H$ NMR spectrum, the typical resonance signals of the CH=CH protons of the vinyl group at $\delta$ = 8.43 (Ru−C*H*=CH) and 5.98 (Ru−CH=C*H*) ppm, along with the presence of the phenylene, dppe and $P^iPr_3$ protons in the correct integral ratios, support the structure with one central bis(ethynyl)ruthenium and two peripheral vinyl ruthenium units. Finally, the IR spectrum reveals the $\nu$(C≡C) band at 2058 $cm^{-1}$ and the $\nu$(C≡O) one at 1910 $cm^{-1}$.

**Crystallographic Studies.** During our studies, X-ray quality crystals of the central bis(arylalkynyl) ruthenium building blocks **2b** and **3b** and of the divinylphenylene bridged complexes $\mathbf{V_a}$ and $\mathbf{V_b}$ have been obtained and their structures were determined. Plots of the structures of **3b** and $\mathbf{V_b}$ are shown in Figures 1 and 2, while those of complexes **2b** and $\mathbf{V_a}$

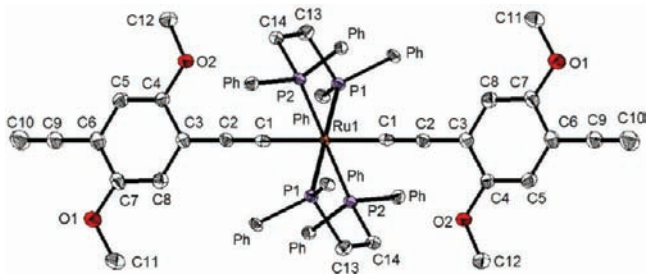


**Figure 1.** Molecular structure of complex **3b**. Cosolvent molecules, dppe phenyl rings, and hydrogen atoms are omitted for clarity; ellipsoids are drawn at a 50% probability level. Selected bond lengths (Å) and angles (deg): Ru−C(1), 2.047(5); C(1)−C(2), 1.223(6); C(9)−C(10), 1.176(7); Ru−P(1), 2.3719(13); Ru−P(2), 2.3317(14) Å; Ru−C(1)−C(2), 177.7(4); C(1)−C(2)−C(3), 177.9(5); C(6)−C(9)−C(10), 179.6(6)°.

can be found in the Supporting Information (Figures S1 and S2), along with tables providing experimental details, the structure solution and refinement, and the atomic positional parameters. Bis(alkynyl) complexes **2b** and **3b** crystallize as centrosymmetric molecules and therefore have strictly linear C−Ru−C arrangements. Ru−C(1)−C(2), C(1)−C(2)−C(3) and C(6)−C(9)−C(10) angles of 177.19(13)/177.7(4), 178.6(2)/177.9(5) and 179.3(2)/179.6(6)° for **2b**/**3b** attest to the nearly ideal rodlike linear arrangement of the entire ruthenium bis(arylethynyl) entity, including the terminal alkynyl group. The C≡C bond lengths of the metal coordinated alkynyl functions of 1.218(2)/1.223(6) Å appear to be slightly longer than those of the terminal unbound alkynyl moieties of 1.207(3) or 1.176(7) Å. The Ru−C bond lengths of 2.0583(17) or 2.047(5) Å present no anomalies from those observed in similar bis(arylalkynyl) complexes of a bis(diphenylphosphino)methane or -ethane $Ru(P_2)_2$ template.[23] In the crystal, individual complex molecules pack in a criss-cross herringbone fashion without any obvious intermolecular contacts other than van der Waals forces.

The structures of complexes $\mathbf{V_a}$ and $\mathbf{V_b}$ closely resemble those of other divinylphenylene bridged diruthenium complexes in many respects such as the planarity of the entire Ru−CH=CH−$C_6H_2R_2$−CH=CH−Ru π-conjugated path and the *cisoid* arrangement of the vinyl and the carbonyl ligands owing to secondary stabilizing interactions between the filled vinyl π- and the empty CO π*-orbitals.[12a,g,24] Specifically, for centrosymmetric complexes $\mathbf{V_a}$/$\mathbf{V_b}$ the Ru−C(1)−C(2)−C(3) torsional angles are −173.4/175.4° while the interplanar angle between the Ru−CH=CH moieties and the phenylene ring amounts to 17.2/18.8°. The Ru−C, C=C and =C−$C_{aryl}$ bond lengths of 1.973(2)/2.002(6), 1.319(4)/1.332(8) and 1.464(3)/1.482(8) Å are also in the usual range. The only obvious difference between the present and the previously reported structures of divinylphenylene bridged diruthenium complexes is difference in the coordination number (five versus six) and coordination geometry (square pyramidal versus octahedral) owing to the


dx.doi.org/10.1021/ic2022177 | *Inorg. Chem.* 2012, 51, 1902−1915

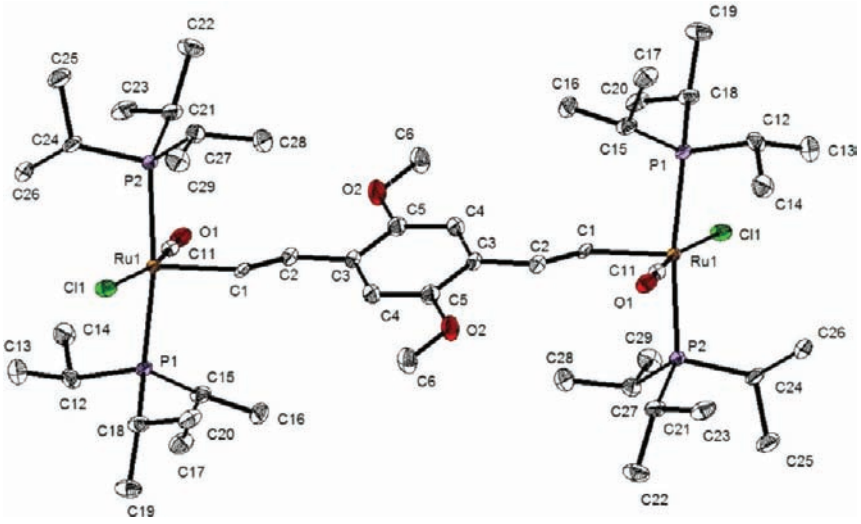


**Figure 2.** Molecular structure of complex $\mathbf{V_b}$. Cosolvent molecules and hydrogen atoms are omitted for clarity; ellipsoids are drawn at a 50% probability level. Selected bond lengths (Å) and angles (deg): Ru−C(1), 2.002(6); Ru−C11, 1.795(6); Ru−Cl(1), 2.4200(18); Ru−P(1), 2.4009(17); Ru−P(2), 2.4036(16); C(1)−C(2), 1.332(8); C(2)−C(3), 1.482(8) Å; Ru−C(1)−C(2), 133.6(5); C(1)−C(2)−C(3), 125.1(4)°.

presence of $RuCl(CO)(P^iPr_3)_2$ instead of $RuCl(CO)(PMe_3)_3$ or $RuCl(CO)(PPh_3)_3$ moieties. The $(RCH{=}CH)RuCl(CO)(P^iPr_3)_2$ unit shows the same structural features as other five-coordinated mononuclear vinyl ruthenium complexes of that unit in that the ruthenium atom is displaced from the plane of the basal ligands toward the apical vinyl ligand. As a consequence the C(1)−Ru−Cl (98.09(8)/107.3(3)°) and C(1)−Ru−P angles (92.3(8) and 96.4(8)/91.35(19) and 94.75(16)°) are appreciably larger than the ideal 90° angle. We note that the Ru−C bond of the vinyl complexes $\mathbf{V_a}/\mathbf{V_b}$ is consistently shorter than that of the alkynyl complexes **2a**/**2b** despite the smaller covalent atomic radius of the sp with respect to the $sp^2$ hybridized carbon atom. This indicates stronger $\pi$-conjugation within the vinyl complexes.

Complexes $\mathbf{V_a}$ as the bis(dichloromethane) solvate and $\mathbf{V_b}$ as the tetrakis(chloroform) solvate also show some interesting features in their packing, and representative views of the unit cell and the hydrogen bonding may be found in the Supporting Information (Figures S3−S5). Thus, molecules of $\mathbf{V_a}$ arrange in rows that run along the crystallographic *c* axis where individual molecules of $\mathbf{V_a}$ are bridged by two $CH_2Cl_2$ solvent molecules through Ru−Cl···$HCCl_2H$···Cl−Ru hydrogen bonds with *d*(H···Cl) = 2.608 and 2.628 Å. For complex $\mathbf{V_b}$, individual molecules also align with their long axis along the crystallographic *c* axis. Two of the four chloroform solvate molecules occupy pockets formed by the chloride ligands and methyl protons of the $P^iPr_3$ ligands with hydrogen bonds of *d*(Ru−Cl···H−$CCl_3$) = 2.628 Å and *d*($H_2CH$···Cl−$CCl_2H$) = 2.916 and 2.944 Å. The other two solvate molecules of the structure, while positioned between the rows, hydrogen bond to the O-atom of the CO ligand of just one complex molecule with *d*(O···H−$CCl_3$) = 2.256 Å.

**Electrochemical Studies.** Cyclic voltammetry (CV) was used to study the electrochemical behavior of **4a,b** ($CH_2Cl_2$, 0.1 M $Bu_4NPF_6$). The values of the potentials are reported in Table 1 along with those of their symmetrical bimetallic counterparts and their monoruthenium bis(arylalkynyl) precursors. Bis(arylalkynyl) complexes **2b** and **3b** present two consecutive one-electron oxidation processes with a large difference of half-wave potentials. While the first oxidation is fully reversible under all conditions, the second becomes so only at sweep rates above 1 V/s or upon cooling to −78 °C (see Supporting Information, Figures S6−S9). This behavior contrasts to that of the nonmethoxy substituted analogues **2a** and **3a**, where no second oxidation was observed. Diruthenium complexes $\mathbf{A_{a,b}}$ and $\mathbf{V_{a,b}}$ present two consecutive, more closely spaced and fully reversible one-electron transfer processes at considerably lower potential due to the presence of an additional electron-rich ruthenium moiety, in full agreement with observations on similar 1,4-diethynyl- or 1,4-divinylphenylene bridged diruthenium or osmium complexes (see Supporting Information, Figures S10 and S11).[10,25] Two points are worth noting: (i) the oxidation potentials of the alkynyl complexes $\mathbf{A_a}$ and $\mathbf{A_b}$ are consistently lower than those of the vinyl complexes $\mathbf{V_a}$ and $\mathbf{V_b}$ owing to the superior donor qualities

**Table 1. Half-Wave Potentials of Complexes 4a,b, of the Parent Complexes 2a,b and 3a,b, and of Symmetrically and Unsymmetrically Bridged Diruthenium Complexes**[a]

| | $E_{1/2}^{0/+}$ [V] | $E_{1/2}^{+/2+}$ [V] | $E_{1/2}^{2+/3+}$ [V] | $E_{1/2}^{3+/4+}$ [V] | $\Delta E_{1/2}$ [mV][b] | $K_c$[c] |
|---|---|---|---|---|---|---|
| **4a** | −0.26[d] | 0.08[d] | 0.26[d] | 0.63[d] | 340 | $5.6 \times 10^5$ |
| | | | | | 180 | $1.1 \times 10^3$ |
| | | | | | 370 | $1.8 \times 10^6$ |
| **4b** | −0.40[d] | −0.08[d] | 0.16[d] | 0.49[d] | 320 | $2.6 \times 10^5$ |
| | | | | | 240 | $1.1 \times 10^4$ |
| | | | | | 330 | $3.8 \times 10^5$ |
| **2b** | −0.11[d] | 0.61[e] | | | 700 | |
| **3a** | 0.01 | | | | | |
| **3b** | −0.09[d] | 0.745[e] | | | 805 | $5.0 \times 10^{13}$ |
| $\mathbf{M_a}$ | −0.22 | 0.14 | | | 360 | $1.2 \times 10^6$ |
| $\mathbf{A_a}$ | −0.33 | 0.01 | | | 340 | $5.6 \times 10^5$ |
| $\mathbf{A_b}$ | −0.495 | −0.10 | | | 395 | $4.0 \times 10^6$ |
| $\mathbf{V_a}$ | −0.075 | 0.175 | | | 250 | $1.7 \times 10^4$ |
| $\mathbf{V_b}$ | −0.215 | 0.06 | | | 275 | $4.5 \times 10^5$ |

[a]Potentials measured in $CH_2Cl_2/NBu_4PF_6$ (0.1 M); potentials are referenced to the $Cp_2Fe^{0/+}$ couple as an internal reference (0.46 V vs SCE), $\Delta E_p$ = 60−70 mV. [b]Difference between half-wave potentials. [c]Comproportionation constant for the reaction $A^{(n+1)+} + A^{(n-1)+} \leftrightarrows 2A^{n+}$ as calculated by the expression $K_c = \exp\{F{\cdot}\Delta E_{1/2}/(R{\cdot}T)\}$. [d]$\Delta E_p$ = 80−90 mV. [e]Half-wave potential at −78 °C where full chemical reversibility was obtained.


dx.doi.org/10.1021/ic2022177 | *Inorg. Chem.* 2012, 51, 1902−1915

of the $RuCl(dppe)_2$ with respect to the $RuCl(CO)(P^iPr_3)_2$ moiety; (ii) the effect of the methoxy substituents is significant for both systems as shown by the shift of half-wave potentials for $\mathbf{A}_{a,b}$ (165 and 110 mV) and $\mathbf{V}_{a,b}$ (140 and 115 mV, respectively). This is a token of large contributions of the carbon-rich bridging ligand to the frontier orbitals of the complexes. Similar differences of $E_{1/2}$ between divinylphenylene bridged diruthenium complexes with or without alkoxy substituents at the phenylene linker were also observed for closely related complexes with $RuCl(CO)(PMe_3)_3$ "caps",[12g,24a] and for ruthenium acetylide complexes.[9a,26]

Typical CVs for **4a,b** are displayed in Figure 3. The trimetallic complexes display three fully reversible one-electron processes at

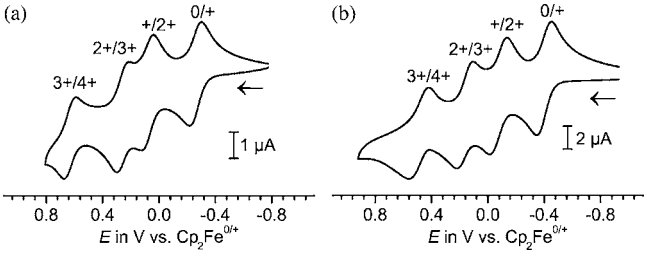


**Figure 3.** CV traces obtained for **4a** (a) and **4b** (b); $Bu_4NPF_6$ (0.1 M) in $CH_2Cl_2$; $v$ = 100 mV·s$^{-1}$.

low potential, in agreement with the number of ruthenium units present in the molecules as observed with related complexes.[8,10] Such events are often erroneously viewed as essentially involving the $Ru^{III}/Ru^{II}$ couple[24a,27] whereas it actually strongly involves the carbon-rich ligands.[8,9,12] An additional chemically reversible (or closely so) process is also observed at higher potential with the lower peak currents most probably ascribed to the smaller diffusion coefficient of the highly charged trication. Comparison of the half-wave potentials of complexes **4a,b** with the mixed complex $\mathbf{M}_a$, the symmetrically substituted acetylide complexes $\mathbf{A}_{a,b}$, and vinylphenylene complexes $\mathbf{V}_{a,b}$ reveals that (i) the half-wave potentials of the first two oxidations are higher than those in the corresponding acetylide complexes $\mathbf{A}_a$ or $\mathbf{A}_b$ but lower than those in the corresponding vinylene complexes $\mathbf{V}_a$ or $\mathbf{V}_b$, (ii) this redox behavior is similar to that of $\mathbf{M}_a$, (iii) the half-wave potential separation between the first and second redox processes resembles that in bis(alkynyl) complexes of the **A** family while that of the second and third oxidations comes close to that in the vinyl bridged complexes $\mathbf{V}_a$ and $\mathbf{V}_b$, and (iv) introduction of a second $C{\equiv}C{-}1,4\text{-}C_6H_2{-}2,5\text{-}R_2{-}CH{=}CH{-}RuCl(CO)(P^iPr_3)_2$ side arm to $\mathbf{M}_a$ increases the number of redox events to a total of four.

Potential separations between the individual half-wave potentials of 180 to 330 mV indicate that the mono-, di-, and trioxidized forms for **4a,b** are thermodynamically stable with respect to disproportionation with comproportionation constants $K_c$ ranging from $1.1 \times 10^3$ to $1.8 \times 10^6$ (Table 1). While this makes them amenable to further studies, the half-wave potential splitting is not a mere reflection of the interaction between the redox centers.[3a,f,28] Nevertheless, it is worth noting that the peripheral vinyl ruthenium sites are way too far apart as to explain the redox-splitting of any of these waves on electrostatic grounds alone. Finally, it is worth noting that introduction of the electron donating methoxy substituents to the phenylene units of the bridging ligands has a substantial effect on all four oxidation potentials of **4b** shifting them cathodically by 140 mV, 160 mV, 100 mV and 140 mV with respect to **4a**, due to the destabilization of HOMO to HOMO−$n$ levels. This suggests again a large participation of these ligands to the redox processes.

**Studies of the Oxidized Species.** In making use of the various spectroscopic tags offered by the ethynyl and vinyl ruthenium subunits, we investigated complexes **4a,b** in every oxidation state, up to the $\mathbf{4a,b}^{4+}$ level, by means of IR, UV−vis−NIR and EPR spectroscopy in order to assign the individual redox processes to the different redox sites and to experimentally probe the electronic coupling between them. For this purpose, the two new bimetallic complexes $\mathbf{A}_b^{n+}$ and $\mathbf{V}_b^{n+}$ ($n$ = 0−2) were also investigated.

**IR and UV−Vis−NIR Spectroelectrochemical Experiments.** The IR properties of the new complexes were first investigated by means of IR spectroelectrochemistry (SEC) in an optically transparent thin-layer electrochemical (OTTLE) cell. Both trimetallic complexes possess the charge sensitive $\nu(C{\equiv}O)$ IR label at the vinyl ruthenium subunit, as well as $\nu(C{\equiv}C)$ and the various combinations of C−H bending and C=C stretching modes of the 1,4-(ethynyl)(vinyl)phenylene subunit that are separately found in the bimetallic $\mathbf{V}_{a,b}$ and $\mathbf{A}_{a,b}$. These labels are indicative of how oxidation affects the charge densities at the vinyl metal terminus and at the bridge. The resulting data are gathered in Table 2 with those of relevant known complexes, and Figures 4 and 5 show the evolution of the IR spectrum of **4a,b** upon electrochemical oxidation. With that in hand, it appears that the IR spectra of $\mathbf{4a,b}^{\bullet+}$, $\mathbf{4a,b}^{2+}$ and $\mathbf{4a,b}^{3+}$ were complicated by the severe overlap of the shifted $\nu(C{\equiv}O)$ and $\nu(C{\equiv}C)$ bands. Comparison of the IR band patterns of $\mathbf{4a,b}^{\bullet+}$ to those of their oxidized precursors $\mathbf{2b}^{\bullet+}$, $\mathbf{3b}^{\bullet+}$ and of $[\{(dppe)_2Ru\}(\mu{-}C{\equiv}C\text{-}1,4\text{-}C_6H_4{-}CH_2{-}SAc)_2]^{\bullet+}$,[10a] where a strong $\nu(C{\equiv}C)$ band is observed at 1889, 1890, and 1902 cm$^{-1}$, respectively, provided first clues as to the heavy involvement of the bis(alkynyl) ruthenium site in the first oxidation process. Some of the remaining ambiguities were then resolved through the $^{13}CO$ labeled analogues **4a*,b***. The labeled hydride complex $RuClH(*CO)(P^iPr_3)_2$ required in this study was prepared by reacting $RuCl_3$ with commercial $^{13}CH_3OH$ in the presence of potassium bicarbonate base and $P^iPr_3$.[29] The achieved labeling level was 91% as inferred from the relative intensities of the $^1H$ NMR signals of the hydride ligand for the two isotopomers with a well resolved doublet of triplet for the $^{13}CO$ (*CO) ($^2J(H,P)$ = 18.30 Hz, $^2J(H,C)$ = 11.54 Hz) but only a triplet ($^2J(H,P)$ = 18.30 Hz) for the $^{12}CO$ isotopomer (CO). $^{12}CO$ replacement by $^{13}CO$ caused a 45 cm$^{-1}$ red shift of the Ru(CO) bands (see Figures 4 and 5). From the comparison of IR spectra of $\mathbf{4a,b}^{\bullet+}$ and of $\mathbf{4a*,b*}^{\bullet+}$, it was clear that the first oxidation of complexes **4a,b** is strongly biased toward the central bis(alkynyl) ruthenium site. Indeed, on removal of one electron, the Ru(CO) band of **4a,b** shifts by only 3−4 cm$^{-1}$ as opposed to 19 cm$^{-1}$ in $\mathbf{M}_a^{\bullet+}$. The shift of $\nu(C{\equiv}C)$ to 1888/1889 cm$^{-1}$ is similar to that of mono-ruthenium bis(acetylide) complexes (*vide supra*) and more pronounced than with $\mathbf{M}_a^{\bullet+}$ and in $\mathbf{A}_{a,b}^{\bullet+}$ in which $\nu(C{\equiv}C)$ is located at ca. 1966 cm$^{-1}$ (see Supporting Information, Figure S12). Thus, replacement of the chloride ligand in $\mathbf{M}_a$ by a second strongly donating $-C{\equiv}C{-}C_6H_2R_2{-}CH{=}CH{-}RuCl(CO)(P^iPr_3)_2$ unit obviously renders the central bis(alkynyl) substituted ruthenium moiety so electron rich that it dominates the first redox event.[30]

While the strong red-shift of the $\nu(C{\equiv}C)$ band of >160 cm$^{-1}$ suggests a large involvement of the central bis(ethynyl) ruthenium moiety in the first oxidation process, the shifts upon


dx.doi.org/10.1021/ic2022177 | Inorg. Chem. 2012, 51, 1902−1915

Table 2. Characteristic IR Data of the Complexes in Various Oxidation States in 0.2 M $NBu_4PF_6$/1,2-$C_2H_4Cl_2$

| | $\tilde{\nu}$(C≡C) [$cm^{-1}$] | $\tilde{\nu}$(C≡O) [$cm^{-1}$] | $\tilde{\nu}$(C=$C_{aryl}$C=$C_{vinyl}$) [$cm^{-1}$] |
|---|---|---|---|
| **4a**[a] | 2058(m) | 1910(s) | 1563(w), 1529(w) |
| **4a**$^{\bullet+}$[a] | 2023(w), 1888(vs) | ~1916(s) | 1579(m), 1529(m), 1512(m), 1492(vs), 1150(vs) |
| **4a**$^{2+}$[a] | 2012(m), 1960(sh), 1860(m) | 1929(vs) | 1579(m), 1529(m), 1512(m), 1492(vs), 1150(vs), 1089(w), 1060(w) |
| **4a**$^{\bullet3+}$[a] | 1775(w) | 1967(s) | 1567(m), 1387(w), 1213(w), 1148(w) |
| **4a** * | 2057(m) | 1864(s) | 1564(w), 1528(w) |
| **4a***$^{\bullet+}$ | 2024(m), 1975(s), 1892(vs) | 1868(vs) | 1578(m), 1528(s), 1514(s), 1490(vs), 1150(vs) |
| **4a***$^{2+}$ | 1990(m), 1960(s), 1860(sh) | 1891(vs) | 1578(m), 1528(s), 1514(s), 1490(vs), 1150(vs), 1089(w), 1060(w) |
| **4a***$^{\bullet3+}$ | 1780(w) | 1925(s) | 1568(m), 1381(w), 1213(w), 1148(w) |
| **4b** | 2052(m) | 1909(s) | 1593(w), 1566(w), 1535(w), 1387(w), 1208(w) |
| **4b**$^{\bullet+}$ | 2034(m), 1889(vs) | 1914(s) | 1588(w), 1543(w), 1500(vs), 1390(s), 1146(s) |
| **4b**$^{2+}$ | 1966(m), 1864(m) | 1932(vs) | 1582(w), 1491(s), 1390(s), 1198(s), 1157(m), 1137(m), 1090(m), 1060(m) |
| **4b**$^{\bullet3+}$ | 2034(w), 1793(m) | 1962(s) | 1793(m), 1189(m), 1133(m), 1090(w), 1060(w) |
| **4b**$^{4+}$ | 2167(w), 1924(m) | 1978(m) | - |
| **4b*** [a] | 2052(w) | 1864(s) | 1593(w), 1566(w), 1535(w) |
| **4b***$^{\bullet+}$[a] | 1966(m), 1890(vs) | 1867(s) | 1588(w), 1543(w), |
| **4b***$^{2+}$[a] | 2026(w), 1865(m) | 1890(vs) | 1586(w), 1540(w) |
| **4b***$^{\bullet3+}$[a] | 2034(w), 1790(w) | 1909(m) | |
| **2b** | 2146(w), 2048(m) | | 1593(w) |
| **2b**$^{\bullet+}$ | 2146(w), 1889(s) | | 1588(w), 1523(w) |
| **3b** | 2050(m) | | 1593(w) |
| **3b**$^{\bullet+}$ | 2049(w), 1890(s) | | 1588(w), 1526(w) |
| $\mathbf{M_a}$ | 2065(m) | 1910(s) | 1565(m), 1527(w), 1497(w), 1486(m), 1482(s) |
| $\mathbf{M_a}^{\bullet+}$ | 2061(w), 1967(m) | 1929(vs) | 1581(m), 1559(m), 1521(m), 1513(m), 1493(s), 1483(m), 1157(vs) |
| $\mathbf{M_a}^{2+}$ | 1888(m) | 1977(s) | 1586(w), 1576(w), 1560(w) |
| $\mathbf{A_a}$[b] | 2071(s) | | |
| $\mathbf{A_a}^{+}$[b] | 2068(m), 1966(vs) | | 1570(s) |
| $\mathbf{A_a}^{2+}$[b] | 1918(s) | | |
| $\mathbf{A_b}$ | 2066(s) | | |
| $\mathbf{A_b}^{+}$ | 2066(w), 1967(s) | | |
| $\mathbf{A_b}^{2+}$ | 2065(w), 1966(m), 1927(m) | | |
| $\mathbf{V_a}$[c] | | 1910 | 1573, 1561 |
| $\mathbf{V_a}^{+}$[c] | | 1932 | 1519, 1503, 1481 |
| $\mathbf{V_a}^{2+}$[c] | | 1991 | |
| $\mathbf{V_b}$ | | 1909(s) | 1558(m), 1388(w), 1206(m), 1128(w), 1091(m) |
| $\mathbf{V_b}^{+}$ | | 1933(s) | 1559(w), 1398(m), 1270(s), 1208(s), 1186(w), 1091(w) |
| $\mathbf{V_b}^{2+}$ | | 1972(s) | 1536(w), 1500(s), 1373(m), 1220(s), 1188(m), 1091(m) |

[a]Only measured in the 2100 to 1510 $cm^{-1}$ range. [b]From ref 10a. [c]From ref 12e.

the second and third oxidations of less than 30 $cm^{-1}$ and of ca. 80 $cm^{-1}$ are more modest. Just the contrary behavior is observed for the Ru(CO) bands: the small blue shift during the first oxidation contrasts to substantially larger ones upon the second and, particularly, the third redox processes (13/18 $cm^{-1}$ and 38/30 $cm^{-1}$ for **4a**/**4b**). For more electron-rich **4b**, even the fourth oxidation could be monitored by IR spectroelectrochemistry. This process was accompanied by a further 16 $cm^{-1}$ blue shift of the Ru(CO) labels as well as a significant blue shift of the alkynyl stretches. The shifts during the second and third oxidation processes are highly reminiscent of those observed in the $\mathbf{M_a}/\mathbf{M_a}^{\bullet+}/\mathbf{M_a}^{2+}$ and the $\mathbf{V_{a,b}}/\mathbf{V_{a,b}}^{\bullet+}/\mathbf{V_{a,b}}^{2+}$ series ($\mathbf{V_b}$: see Supporting Information, Figure S14). Most importantly, our results indicate that **4a,b**$^{n+}$ and **4a*,b***$^{n+}$ have just *one single* Ru(CO) band in their IR spectra such that both C≡C−$C_6H_2R_2$−CH=CH−RuCl(CO)($P^iPr_3$)$_2$ "side arms" remain electronically equivalent throughout the entire **4a**$^{0\rightarrow3+}$ or **4b**$^{0\rightarrow4+}$ redox series. This shows that all relevant frontier molecular orbitals are fully delocalized over the entire {Ru′}−CH=CH−$C_6H_2R_2$−C≡C−{Ru}−C≡C−$C_6H_2R_2$−CH=CH−{Ru′} array, though involving the central and peripheral parts of the structure to a differing degree. From the similar $\nu$(CO) IR band positions, we also conclude that both vinyl ruthenium arms in **4a**$^{2+}$ and **4a**$^{3+}$ have about the same charge densities as in their bimetallic counterparts $\mathbf{M_a}^{\bullet+}$ and $\mathbf{M_a}^{2+}$ and $\mathbf{V_{a,b}}^{\bullet+}/\mathbf{V_{a,b}}^{2+}$. These latter radical cations have both been found to be strongly delocalized systems, and this is also the case for **4a,b**$^{n+}$ ($n$ = 1, 2, 3). In addition, we note that (i) the growth of intense phenylene based absorptions in the 1580 to 1490 $cm^{-1}$ range and of a band at 1150 $cm^{-1}$ during the first and second oxidations is a token of the strong participation of the bridge to the overall oxidation process as in $\mathbf{M_a}$, and (ii) the intensities of the $\nu$(C≡C) and phenylene vibrations strongly decrease upon the third oxidation, possibly as a result of a weaker change in dipolar moment upon vibration in this highly charged species as was observed for other charged trimetallic acetylides.[10a] We are thus dealing with highly bridge-centered radical cations with the positive charges almost evenly delocalized over the entire $\pi$-conjugated bis(vinyl)(ethynyl)-phenylene triruthenium backbone. We also note that the total Ru(CO) band shift in the redox series **4b** → **4b**$^{3+}$ of 53 $cm^{-1}$ is somewhat smaller than that of 57 $cm^{-1}$ for the **4a** → **4a**$^{3+}$ series, which may indicate a slightly but not significantly larger participation of the more electron-rich bridging ligand to the


dx.doi.org/10.1021/ic2022177 | Inorg. Chem. 2012, 51, 1902−1915

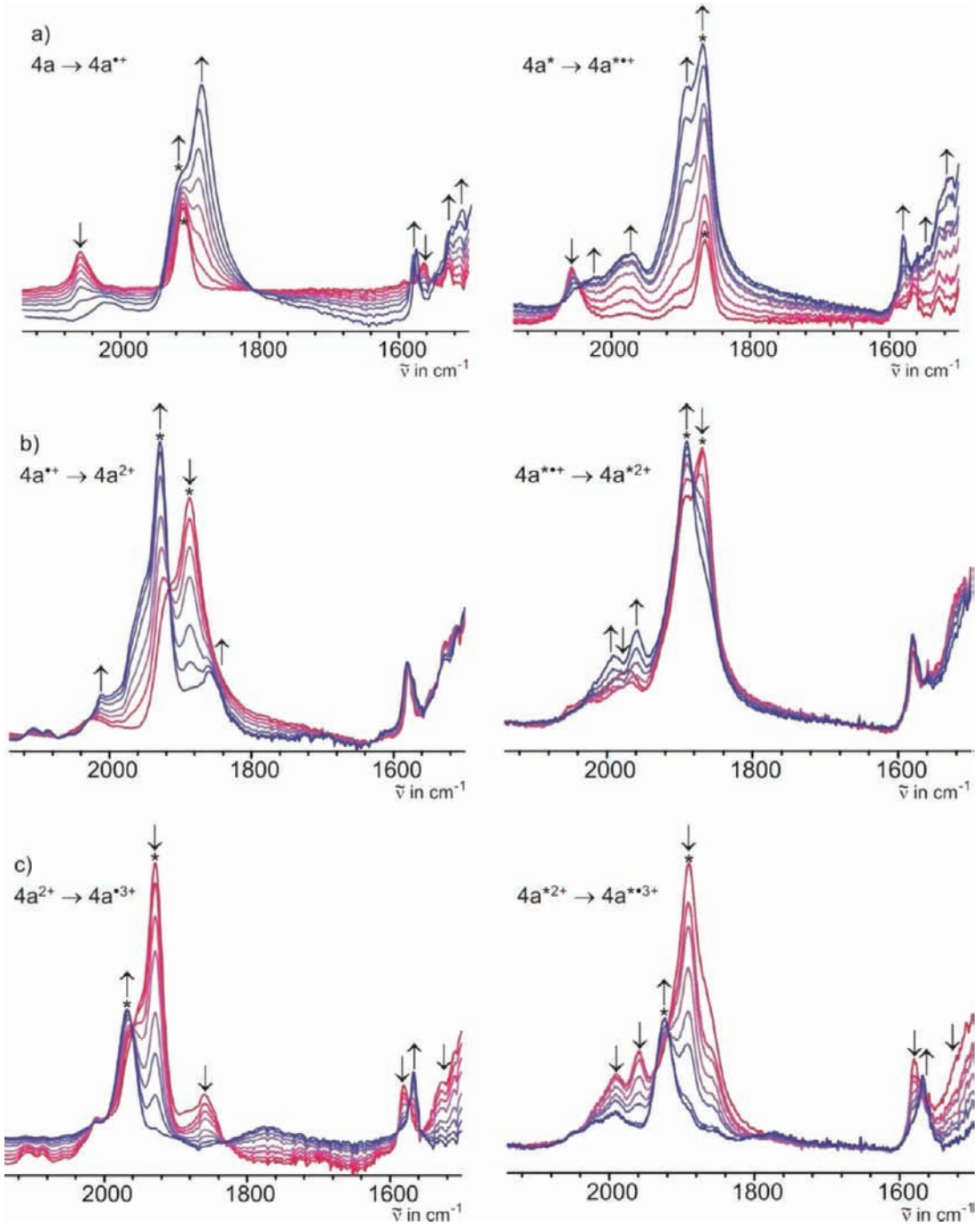


**Figure 4.** IR-spectroscopic changes of **4a** (left) and **4a*** (right) during the first (a), second (b) and third oxidation (c) in 0.2 M $NBu_4PF_6$/1,2-$C_2H_4Cl_2$. The CO band of each species is indicated by the asterisk symbol (*).

already highly ligand centered oxidation processes. Interestingly, $\mathbf{V_b}$ and $\mathbf{V_a}$ show a similar charge distribution in the first oxidized state but a somewhat more ligand centered process for the dimethoxy-substituted $\mathbf{V_b}$ in the second event, as attested by a smaller CO band shift (39 $cm^{-1}$ vs 59 $cm^{-1}$).

More evidence toward full delocalization comes from the electronic spectra (Table 3, Figure 6). In addition to the intense short-wavelength absorption bands for transitions involving the phosphine ligands (intraligand transitions), the trimetallic complexes **4a,b** show a broad absorption band with a large extinction coefficient at lower energy at around 380−400 nm. This transition should be a multiconfigurational MLCT excitation resulting from a considerable mixing of Ru(d$\pi$) orbitals with alkynyl/vinyl $\pi$-orbitals and should present a $Ru^{II}(d\pi) \rightarrow \pi^*(L)$ (MLCT) character admixed with a strong $\pi \rightarrow \pi^*$ (IL) nature (Figure 6).[3f,9a,12b,31] As previously observed for similar ruthenium acetylide complexes and for $\mathbf{V_b}$, the methoxy substituents induce a red shift of the main band (ca. 20−40 nm, see also Supporting Information, Figure S15).[26,17] Upon oxidation in the OTTLE cell, this transition vanishes, and the radical cations $\mathbf{4a,b^{\bullet+}}$ present an intense low-energy absorption band at ca. 1600 nm, obviously composed of several transitions. These bands are unlikely IVCT transitions for this kind of complex and are assigned as SOMO−$n$ → SOMO transitions in


dx.doi.org/10.1021/ic2022177 | Inorg. Chem. 2012, 51, 1902−1915

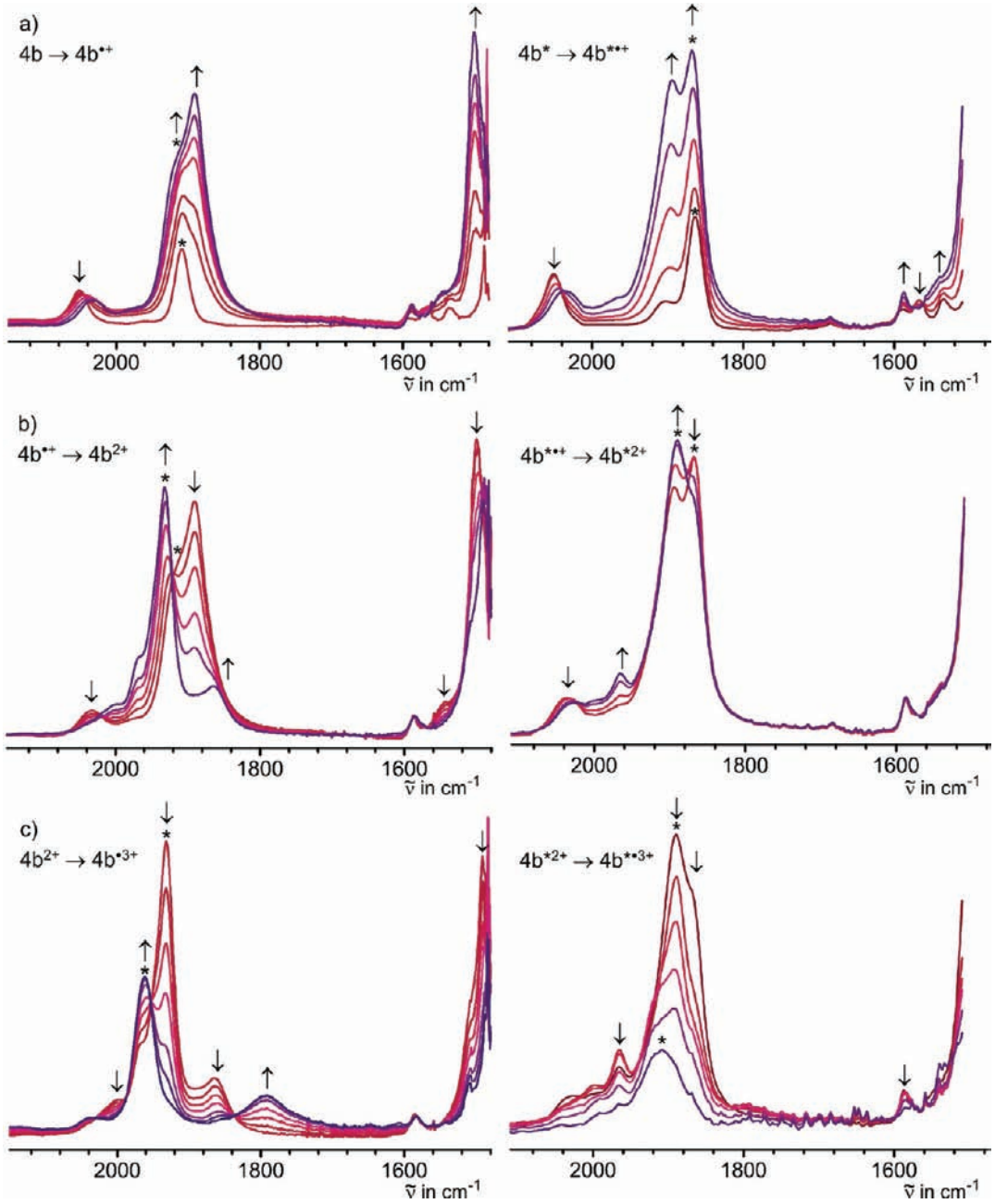


**Figure 5.** IR-spectroscopic changes of **4b** (left) and **4b*** (right) during the first (a), second (b) and third oxidation (c) in 0.2 M $NBu_4PF_6$/1,2-$C_2H_4Cl_2$. The CO band of each species is indicated by the asterisk symbol (*).

a complex manifold within an extended $\pi$-conjugated open shell complex.[32] While involving some charge transfer from the metal groups to the central arene part of the bridges, there is certainly a strong $\pi \rightarrow \pi^*$ (IL) character as revealed by their close resemblance to those of oxidized purely organic counterparts.[33] This notion finds additional support from our EPR studies, which also point out the fact that this process is far from being fully metallic and involves mainly the organic ligands (*vide infra*). These "radical bands" are located at lower energies than those found for $[Ph{-}C{\equiv}C{-}Ru(dppe)_2{-}C{\equiv}C{-}C_6H_4{-}C{\equiv}CH]^{\bullet+}$ ($\lambda_{max}$ = 1157 nm)[17] and the methoxy substituted precursors $\mathbf{2b}^{\bullet+}$ and $\mathbf{3b}^{\bullet+}$ (1372, 1350 nm, see Supporting Information, Figures S18 and S20) and those observed for $\mathbf{M_a}^{\bullet+}$ (1340 nm) and, interestingly, its phenylethynyl substituted derivative $[(PhC{\equiv}C{-}Ru(dppe)_2{-}C{\equiv}C{-}C_6H_4{-}CH{=}CH{-}RuCl(CO)(P^iPr_3)_2]^{\bullet+}$ ($\mathbf{M_{ph}}^{\bullet+}$, 1491 nm).[17] In addition, the low energy features are similar in shape to the latter (alkynyl)(vinyl)phenylene-bridged radical cations. This is consistent with the spreading of the involved orbitals over both alkynyl ligands including the vinylene units. The contribution of both sides in bis(acetylides) was already pointed out with the fact that for $[Ph{-}C{\equiv}C{-}Ru(dppe)_2{-}C{\equiv}C{-}C_6H_4{-}C{\equiv}CH]^{\bullet+}$ the low energy transition occurs at considerably lower energy than that of its chloro-terminated counterpart $[Cl{-}Ru(dppe)_2{-}C{\equiv}C{-}C_6H_4{-}C{\equiv}CH]^{\bullet+}$.[17] Upon the second oxidation to $\mathbf{4a,b}^{2+}$, new transitions appear on the low energy side of the low energy band (**4a,b**) and intensify (**4b**). During the third oxidation to $\mathbf{4a,b}^{3+}$, the low energy bands vanish and a series of overlapping bands in their NIR and visible spectra leads to plateaulike absorption over the high energy side of the previous bands to ca. 1300 nm. This may indicate transitions from a larger manifold


dx.doi.org/10.1021/ic2022177 | *Inorg. Chem.* 2012, 51, 1902–1915

**Table 3. Characteristic UV/Vis/NIR Data in Various Oxidation States in 0.2 M $NBu_4PF_6$/1,2-$C_2H_4Cl_2$**

| | $\lambda_{max}$ [nm] (energy [$cm^{-1}$]; $\varepsilon$ [$M^{-1}$ $cm^{-1}$]) |
|---|---|
| **4a** | 383 (26110; 69500), 517 (19342; 2050) |
| $\mathbf{4a}^{\bullet+}$ | 355 (28169; 30040), 531 (18832; 18800), 1586 (6305; 21510) |
| $\mathbf{4a}^{2+}$ | 341 (29326; 22400), 526 (19011; 20000), 725 (13793; 7350), 1616 (6188; 26400), ~2000 (5000; 17350) |
| $\mathbf{4a}^{\bullet3+}$ | 646 (15480; 18150), 1145 (8734; 23300) |
| **4b** | 308 (32450; 30000), 400 (25003; 70000), 549 (2400) |
| $\mathbf{4b}^{\bullet+}$ | 304 (32880; sh), 370 (26993; 40000), 557 (17948; 34000), 1154 (8665; sh), 1610 (6285; 34000) |
| $\mathbf{4b}^{2+}$ | 366 (27350; 23000), 538 (18600; 40000), 1490 (6700; 49000), 1920 (5205; 54000) |
| $\mathbf{4b}^{3+}$ | 363 (27550; 16500), 488 (20500; 20800), 543 (18430; 21800), 739 (13525; 36000), 1193 (8380, 67000) |
| $\mathbf{4b}^{4+}$ | 383 (26108; 19000), 732 (13660; 40000), 889 (11140; 47000), 1010 (9900; 64000) |
| **2b** | 410 (24390; 68250) |
| $\mathbf{2b}^{\bullet+}$ | 348 (28735; 24 012), 413 (24213; 27540), 1372 (7289; 21956) |
| **3b** | 402 (24876; 58930) |
| $\mathbf{3b}^{\bullet+}$ | 345 (33693; 29860), 406, (24630; 32000), 498 (20080; 10400), 1350 (7407; 21100) |
| $\mathbf{M_a}$ | 368 (27174; 32500) |
| $\mathbf{M_a}^{\bullet+}$ | 525 (19048; 20200), 1340 (7463; 33000) |
| $\mathbf{M_a}^{2+}$ | 400 (25000; 6200), 719 (13908; 35700) |
| $\mathbf{A_b}$ | 388(25773; 111900) |
| $\mathbf{A_b}^{+}$ | 504 (19841; 62100), 560 (17857; 98700), 1180 (8475; 41300) (sh), 1380 (7246; 130900) |
| $\mathbf{A_b}^{2+}$ | 570 (17544; 30900) (sh), 844 (11848; 119000) |
| $\mathbf{V_b}$ | 379 (26385; 41500), 548 (18248; 1500) |
| $\mathbf{V_b}^{+}$ | 374 (26738; 14700), 557 (17953; sh), 602 (16610; 32300), 877 (11400; sh), 1002 (9980; 15100), 1153 (8673, 33600) |
| $\mathbf{V_b}^{2+}$ | 371 (26954; 10700), 503 (19880; sh), 660 (15151; 45000) |

of lower-lying occupied donor orbitals spreading over the entire conjugated path into the emptied bridge-based, delocalized frontier orbitals as it was observed for $[(PhC{\equiv}C{-}Ru(dppe)_2{-}C{\equiv}C{-}C_6H_4{-}CH{=}CH{-}RuCl(CO)(P^iPr_3)_2]^{2+}$ ($\mathbf{M_{ph}}^{2+}$), albeit in a more restricted range. As with IR spectroelectrochemistry, the introduction of two electron donating methoxy groups into the bridging ligands allowed us to also study the fourth oxidation process under UV−vis−NIR monitoring. This final process led to a further blue shift of all electronic bands while maintaining their overall pattern and absorbances.

**EPR Spectroscopy.** In order to get further insight into the electronic structure of paramagnetic species, EPR spectroscopy is particularly instructive. It has been much used as an empirical rule that the principal values and the anisotropy of the *g*-tensor may be considered as a qualitative indicator of the spin densities at the metal and the organic ligand(s), i.e. the metal/ligand character of the odd-electron species. A larger metal contribution generally leads to a larger departure of the *g*-value from that of the free electron and larger *g*-anisotropies.[34] Accordingly, smaller *g* anisotropies and an average $\langle g \rangle$ closer to the free electron *g*-value ($g_e$) suggest a larger organic $\pi$-orbital character of the unpaired electron. This fact was recently observed and supported by theoretical calculations on the acetylide and vinyl systems of interest here.[3f,9a] In addition, as rapid relaxation often renders Ru(III) species ESR silent in fluid solution, intense isotropic EPR signals at RT make therefore a strong case for ligand-dominated oxidation.

The EPR signal of chemically generated $\mathbf{A_b}^{\bullet+}$ shows identical features to those of a $\mathbf{A_a}^{\bullet+}$ in solution with an isotropic and broad signal at room temperature with $g$ = 2.047 and no resolved hyperfine splitting (Table 4) (see Supporting Information, Figure S25). In contrast, the low-temperature spectrum exhibits rhombic symmetry with no hyperfine splitting and a calculated *g* value $\langle g_{av} \rangle$ = 2.042 and $\Delta g$ = 0.120. This means that the spin density of the single electron is distributed over the bridge and the metal centers, with a slightly larger ligand participation with this more electron-rich ligand than in $\mathbf{A_a}^{\bullet+}$ and with relatively little metal contribution, as expected.[9a]

The EPR signal of chemically or electrochemically generated $\mathbf{V_b}^{\bullet+}$ is isotropic in fluid or frozen solution and in the solid state with its *g* value of 2.0155 (see Supporting Information, Figure S26). This value is even closer to the free electron value than with $\mathbf{V_a}^{\bullet+}$ ($g$ = 2.0278),[12e] thus also emphasizing a slightly more ligand centered oxidation. The EPR spectrum in fluid solution is quite well resolved with $g_{iso}$ = 2.0208 (Figure 7). External lines in the wings of the EPR spectra are due the hyperfine splitting (hfs) of the $^{99/101}$Ru isotopes. If the electron is well delocalized over the two metal centers, the active set of nuclei being considered should be $^{31}$P (4 P), $^{99,101}$Ru (2 Ru). With these guidelines, the observed EPR spectrum of $\mathbf{V_b}^{\bullet+}$ could be properly simulated (Figure 7).

Samples of the monooxidized paramagnetic $\mathbf{4a,b}^{\bullet+}$ species were obtained *via* chemical oxidation of **4a** with ferrocenium hexafluorophosphate in $CH_2Cl_2$ and via electrochemical oxidation for **4b**, at RT and 103 K, and their EPR spectra recorded (Figures 8 and 9, Table 4). They are almost fully isotropic and centered at *g* values similar to those observed for the mixed systems $\mathbf{M_a}^{\bullet+}$ and $\mathbf{M_{ph}}^{\bullet+}$, also evidencing the dominant organic character with the major spin densities on the bridging ligands, and an intermediate behavior between the $\mathbf{A_{a,b}}^{\bullet+}/\mathbf{V_{a,b}}^{\bullet+}$ series. These observations support the results from IR spectroelectrochemistry giving the picture of monooxidized species with a single electron mainly delocalized on the central bis(alkynyl) unit and, as expected, with a more pronounced ligand character than in the bis(alkynyl) precursor cation $\mathbf{3b}^{\bullet+}$ that displays slightly higher *g* values and a rhombic signal with a larger anisotropy in frozen solution.

**Concluding Remarks.** In this work, we have synthesized two novel trimetallic ruthenium carbon-rich compounds with (ethynyl)(vinyl)phenylene bridging motifs for molecular electronics that provide a large conduit for electron delocalization. The study of these complexes suggests that they are a fascinating case of trinuclear complexes exhibiting strong electron delocalization over three redox-active subunits in up to five different oxidation states, and that the two bridges are noninnocent redox-active ligands which cannot be decoupled from the metals in any of the redox processes. More specifically, with the help of electrochemical and spectroscopic (UV−vis−NIR−IR and EPR) techniques, we show that upon one-electron oxidation ($n$ = 1) the single unpaired electron is uniformly delocalized over the two carbon chains, mainly around the central metal atom. Interestingly, the studies on the triruthenium complex **4a,b** and comparison with the diruthenium complex $\mathbf{M_a}$ have indicated that introduction of the second electron-rich $C{\equiv}C{-}C_6H_4{-}CH{=}CH{-}RuCl(CO)(P^iPr_3)_2$ moiety preferentially lowers the energy at the central bis(alkynyl) site. This obviously decreases the contribution of the peripheral vinyl ruthenium sites to the SOMO in $\mathbf{4a,b}^{\bullet+}$ such that it is less delocalized over the $\{Ru\}{-}C{\equiv}C{-}C_6H_2R_2{-}CH{=}CH{-}\{Ru'\}$ arms than it is the case for $\mathbf{M_a}^{\bullet+}$. In contrast, the second and the third oxidations ($n$ = 2, 3) involve the whole carbon-rich conjugated path of the molecule with the positive charges uniformly distributed along the entire $\pi$-conjugated $Ru{-}CH{=}CH{-}C_6H_2R_2C{\equiv}C{-}Ru{-}C{\equiv}C{-}C_6H_2R_2CH{=}CH{-}Ru$


dx.doi.org/10.1021/ic2022177 | Inorg. Chem. 2012, 51, 1902−1915

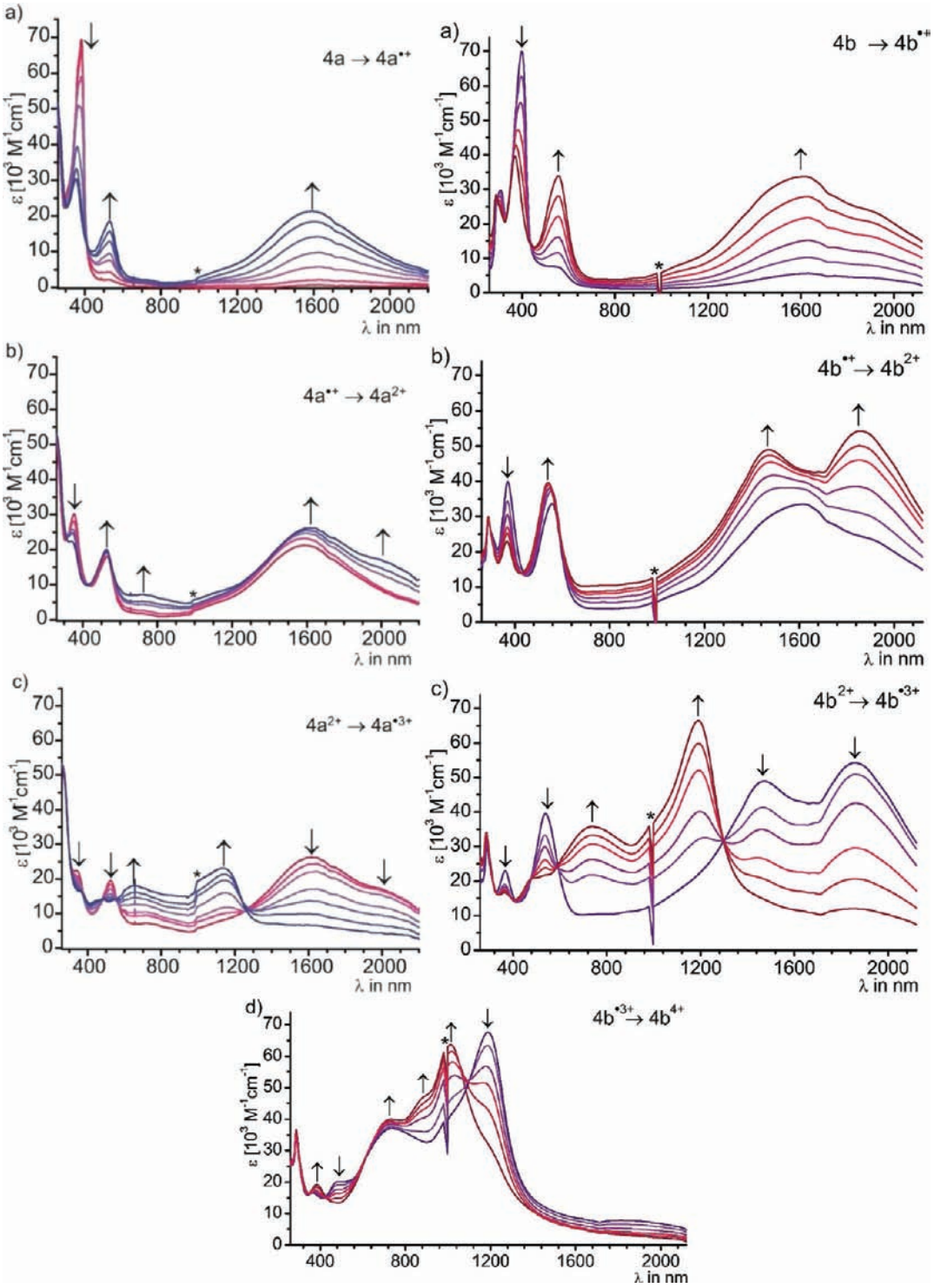


**Figure 6.** UV/vis/NIR-spectral changes of **4a** (left) and **4b** (right) during first (a), second (b), third (c), and fourth (d) oxidations in 0.2 M $NBu_4PF_6$ /1,2-$C_2H_4Cl_2$. The asterisk symbol (*) indicates discontinuities due to instrument and detector change.

backbone as it is the case for the oxidized diruthenium complex $\mathbf{M_a}$, and therefore with a larger ligand contribution than in the trimetallic systems containing the $[RuCl_n(dppe)_2]$ ($n$ = 0, 1) fragment only.

In order to try to further increase both the contribution of the peripheral sites and electron delocalization over the entire {Ru′}−bridge−{Ru}−bridge−{Ru′} array, we attached electron donating substituents to the bridging phenylene units, owing to the larger contribution of the phenyl substituent to the local redox orbitals of ruthenium styryl when compared to ruthenium phenylethynyl complexes. The introduction of two methoxy substituents in the bridging arylene units lowers each oxidation potential by 100 to 160 mV and renders **4b** so electron-rich that even the tetraoxidized $\mathbf{4b}^{4+}$ could be identified by different spectroscopies. Nevertheless, surprisingly, the slightly lower CO band shifts of $\mathbf{4b}^{n+}$ compared to those in the $\mathbf{4a}^{n+}$ series indicate only a slightly larger participation of the more electron-rich bridging ligand to these already highly ligand


dx.doi.org/10.1021/ic2022177 | Inorg. Chem. 2012, 51, 1902−1915

**Table 4. EPR Data at Room Temperature and at 103 K in Solution ($CH_2Cl_2$) and the Solid State**

| | | $T$ = RT | $T$ = 103 K |
|---|---|---|---|
| $\mathbf{A_a}^{\bullet+}$ [a] | solution | $g_{iso}$ = 2.0469 (THF) | $g_1$ = 2.155, $g_2$ = 2.052, $g_3$ = 1.992 $\Delta g$ = 0.163, $\langle g_{av}\rangle$ = 2.067 (THF) |
| $\mathbf{A_b}^{\bullet+}$ | solution | $g_{iso}$ = 2.047 | $g_1$ = 2.106, $g_2$ = 2.033, $g_3$ = 1.986 $\Delta g$ = 0.120, $\langle g_{av}\rangle$ = 2.042 |
| $\mathbf{3b}^{\bullet+}$ | solution | $g_{iso}$ = 2.042 | $g_1$ = 2.100, $g_2$ = 2.033, $g_3$ = 1.986 $\Delta g$ = 0.114, $\langle g_{av}\rangle$ = 2.040 |
| $\mathbf{V_a}^{\bullet+}$ [b] | solution | $g_{iso}$ = 2.0278 ($A(^1H)$ = 9.2 (2H), 8 (2H) G; $A(^{99/101}Ru)$ = 4.5 G) | $g_{iso}$ = 2.0221 |
| $\mathbf{V_b}^{\bullet+}$ | solution | $g_{iso}$ = 2.0208 ($A(^{31}P)$ = 9.2 G; $A(^{99/101}Ru)$ = 4.7 G)[c] | $g_{iso}$ = 2.0150 |
| | solid | $g_{iso}$ = 2.0155 | $g_{iso}$ = 2.0155 |
| $\mathbf{M_a}^{\bullet+}$ | solution | no signal | $g_{iso}$ = 2.0191 |
| | solid | $g_{iso}$ = 2.0289 | $g_{iso}$ = 2.0327 |
| $\mathbf{M_{Ph}}^{\bullet+}$ | solution | $g_{iso}$ = 2.0568 | $g_\perp$ = 2.1290, $g_\parallel$ = 2.0176,[c] $\Delta g$ = 0.111, $\langle g_{av}\rangle$ = 2.0554 |
| | solid | $g_{iso}$ = 2.0365 | $g_{iso}$ = 2.0383 |
| $\mathbf{4a}^{\bullet+}$ | solution | no signal | $g_{iso}$ = 2.0177 |
| | solid | $g_{iso}$ = 2.0301 | $g_{iso}$ = 2.0320 |
| $\mathbf{4b}^{\bullet+}$ | solution | $g_{iso}$ = 2.033 | $g_\perp$ = 2.029, $g_\parallel$ = 1.994, $\Delta g$ = 0.035, $\langle g_{av}\rangle$ = 2.017 |

[a]From ref 10a. [b]From ref 12e. The hyperfine splitting in this reference is somewhat ambiguous since an equally good fit can be obtained by assuming coupling to four $^{31}P$ nuclei by 9.0 G. [c]Data based on the spectrum simulation.

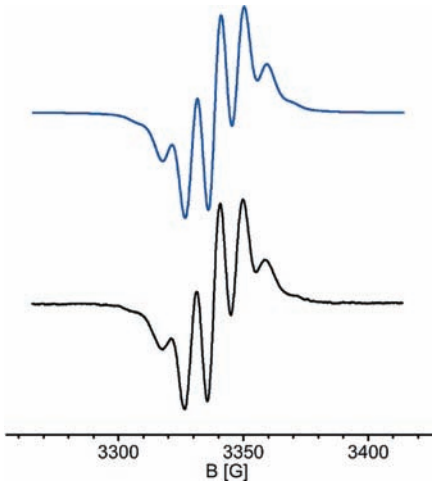


**Figure 7.** First derivative EPR spectra of $\mathbf{V_b}^{\bullet+}$. Lower trace: experiment recorded at RT (solution). Upper trace: computer simulation with $A(^{31}P)$ = 9.2 G (4 P), $A(^{99/101}Ru)$ = 4.7 G (2 Ru).

centered oxidation processes, a fact also observed for the bimetallic counterparts $\mathbf{A_{a/b}}$ and $\mathbf{V_{a/b}}$ with EPR spectroscopy. Note that this Ru(CO) IR probe turned out to be a particularly

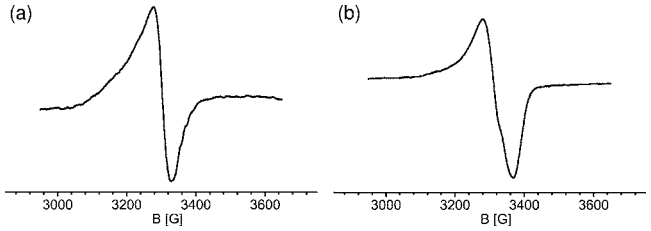


**Figure 9.** First derivative EPR spectra of $\mathbf{4b}^{\bullet+}$ in $CH_2Cl_2$ solution at RT (a) and in frozen solution at 103 K (b).

valuable tool to assess the charge distribution in different oxidation states, and $^{13}CO$ labeled analogues **4a*,b*** allowed us to disseminate overlapping vibration stretches due to the acetylide triple bonds and to the intense and charge-sensitive CO probe. In particular, from these studies we were able to establish that the peripheral CO bearing vinyl ruthenium sites remain electronically equivalent throughout the entire $\mathbf{4a}^{0\rightarrow3+}$ or $\mathbf{4b}^{0\rightarrow4+}$ series.

Because molecular wires display properties strongly connected to their structure, and understanding of charge transport through molecular wires in metal−molecule−metal junctions is a central issue,[35] such redox-active carbon-rich metal complexes allowing intramolecular electron transfer with easily accessible and interconvertible redox states are objects of special interest.[16] Via addition of electrode linking units on the terminal moieties, they will give valuable insights into the structure−property relationships of molecular junctions with hole-conducting properties and low turn-on voltage.

## EXPERIMENTAL SECTION

All manipulations were performed with standard Schlenk techniques under argon or nitrogen atmosphere. Solvents were dried by standard procedures and degassed by saturation with argon or nitrogen prior to use. Infrared spectra were obtained on a Perkin-Elmer Paragon 1000 PC FT-IR or a Thermo is10 instrument. $^1H$, $^{13}C$ and $^{31}P$ NMR spectra were recorded on either a Bruker AC 250, a Bruker Avance III 400, a Bruker Avance III Kryo-Platform 600 MHz or a Varian Unity INOVA 400 spectrometer in $CDCl_3$ or $CD_2Cl_2$ solutions at 303 K. The spectra were referenced to the residual protonated solvent ($^1H$), the solvent signal itself ($^{13}C$) or external $H_3PO_4$ ($^{31}P$). The assignment of $^{13}C$ NMR signals was aided by HSQC and HMBC experiments. UV/vis spectra were obtained on an Omega 10 spectrometer from Bruins Instruments or a TIDAS fiberorptic diode array spectrometer (combined MCS UV/NIR and PGS NIR instrumentation) from j&m in HELLMA quartz cuvettes with 1 cm optical path lengths. Elemental analyses (C,H,N) were performed at in-house facilities. HR-MS spectra were recorded on a Bruker MicrO-Tof-Q 2 spectrometer. The equipment for voltammetric and spectroelectrochemical studies and the conditions employed in this work was as described elsewhere.[36] Electron paramagnetic resonance (EPR) studies were performed on a table-top X-band spectrometer Miniscope from Magnettech. X-ray measurements were performed at 100(2) K with a crystal mounted on a glass fiber on a Stoe IPDS II diffractometer (graphite monochromator, Mo K$\alpha$ radiation, $\lambda$ = 0.710 73 Å). The structures were

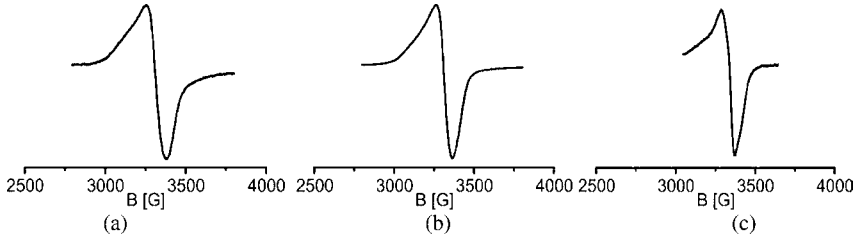


**Figure 8.** First derivative EPR spectra recorded at $\mathbf{4a}^{\bullet+}$ as solid at RT (a), as a solid at 103 K (b) and in frozen $CH_2Cl_2$ solution at 103 K (c).


dx.doi.org/10.1021/ic2022177 | Inorg. Chem. 2012, 51, 1902−1915

solved by direct methods using the SHELX-97 program package.[37] The positions of the hydrogen atoms were calculated by assuming an ideal geometry, and their coordinates were refined together with those of the attached carbon atoms as the riding model. All other atoms were refined anisotropically. Complexes *trans*-(dppe)$_2$Ru(−C≡C-*p*-C$_6$H$_4$−C≡C−H (**3a**),[18] [(dppe)$_2$RuCl](OTf),[38] *cis*-(dppe)$_2$RuCl$_2$,[39] and RuClH(CO)(P$^i$Pr$_3$)$_2$[19] were synthesized by known procedures.

***trans*-[{Ru(dppe)$_2$}{μ-C≡C-1,4-C$_6$H$_2$−2,5-(OMe)$_2$−C≡C−SiMe$_3$}$_2$] (2b).** Ru(dppe)$_2$Cl$_2$ (0.180 g, 0.19 mmol) and NaPF$_6$ (0.125 mg, 0.74 mmol) were treated with 10 mL of CH$_2$Cl$_2$ under a nitrogen atmosphere. A solution of 1-ethynyl-2,5-dimethoxy-4-[2-(trimethylsilyl)ethynyl]benzene (0.106 g, 0.41 mmol) and NEt$_3$ (0.515 mL, 3.72 mmol) in 10 mL of CH$_2$Cl$_2$ was slowly added. The solution was stirred for 16 h at RT, and volatiles were removed in vacuum afterward. The crude product was dissolved in the minimum volume of THF. After performing a column chromatography (Al$_2$O$_3$) with Et$_2$O, the solid obtained after evaporating the solvent was taken up in 2 mL of CH$_2$Cl$_2$ and treated with 20 mL of *n*-hexane whereupon the product precipitated. After the precipitate was washed with 5 mL of *n*-hexane twice and dried in vacuum, the product was obtained as a yellow-colored solid. Yield: 0.248 mg (92%). $^1$H NMR (400 MHz, CD$_2$Cl$_2$): δ 7.50−7.43 (m, 16H, *o*-C$_6$H$_5$ (dppe)), 7.12 (t, 8H, $^3J$(H,H) = 7.3 Hz, *p*-C$_6$H$_5$ (dppe)), 6.89 (t, 16H, $^3J$(H,H) = 7.5 Hz, *m*-C$_6$H$_5$ (dppe)), 6.83 (s, 2H, C$_6$H$_2$(OMe)$_2$), 5.88 (s, 2H, C$_6$H$_2$(OMe)$_2$), 3.71 (s, 6H, OCH$_3$), 3.63 (s, 6H, OCH$_3$), 2.93−2.85 (m, 8H, PCH$_2$CH$_2$P), 0.28 (s, 18H, SiMe$_3$). $^{13}$C{$^1$H} NMR (100 MHz, CD$_2$Cl$_2$): δ 155.0, 154.3 (each s, COMe/C$_6$H$_2$(OMe)$_2$), 142.9 (m, Ru−C≡C), 137.9 (m, *ipso*-C$_6$H$_5$ (dppe)), 134.8−134.7 (m, *o*-C$_6$H$_5$ (dppe)), 129.1 (s, *p*-C$_6$H$_5$ (dppe)), 127.5−127.4 (m, *m*-C$_6$H$_5$ (dppe)), 122.7 (s), 115.8 (s), 115.3 (s), 114.9 (s), 106.2 (s), 103.6 (s, C≡C−Si), 97.8 (s, C≡C−Si), 56.5 (s, OCH$_3$), 56.4 (s, OCH$_3$), 31.7 (m, |$^1J$(C,P) + $^3J$(C,P)| = 23 Hz, PCH$_2$CH$_2$P), 0.5 (s, SiMe$_3$). $^{31}$P{$^1$H} NMR (161 MHz, CD$_2$Cl$_2$): δ 53.33 (s, dppe). FT-IR (cm$^{-1}$, ATR) = 2141 (m, ν$_{C≡CSi}$), 2045 (s, ν$_{C≡CRu}$).

***trans*-[{Ru(dppe)$_2$}{μ-C≡C-1,4-C$_6$H$_2$−2,5-(OMe)$_2$−C≡CH}$_2$] (3b).** *trans*-[{Ru(dppe)$_2$}{μ-C≡C-1,4-C$_6$H$_2$−2,5-(OMe)$_2$−C≡C−SiMe$_3$}$_2$] (**2b**, 0.248 g, 0.18 mmol) was dissolved in 15 mL of THF under a nitrogen atmosphere. A 1 M solution of Bu$_4$NF in THF (0.380 mL, 0.38 mmol) was slowly added. The solution was stirred for 1.5 h at RT, after which time the solvent was removed under vacuum. The crude product was washed twice with 10 mL of H$_2$O. The product was taken up in 2 mL of CH$_2$Cl$_2$ and then precipitated by addition of 20 mL of MeOH. After the precipitate was washed with 5 mL of MeOH twice and dried in vacuum, the product was obtained as a yellow-colored solid. Yield: 0.185 g (81%). $^1$H NMR (400 MHz, CD$_2$Cl$_2$): δ 7.49−7.44 (m, 16H, *o*-C$_6$H$_5$ (dppe)), 7.12 (t, 8H, $^3J$(H,H) = 7.3 Hz, *p*-C$_6$H$_5$ (dppe)), 6.89 (t, 16H, $^3J$(H,H) = 7.5 Hz, *m*-C$_6$H$_5$ (dppe)), 6.86 (s, 2H, C$_6$H$_2$(OMe)$_2$), 5.90 (s, 2H, C$_6$H$_2$(OMe)$_2$), 3.70 (s, 6H, OCH$_3$), 3.63 (s, 6H, OCH$_3$), 3.32 (s, 2H, C≡CH), 2.93−2.86 (m, 8H, PCH$_2$CH$_2$P). $^{13}$C{$^1$H} NMR (100 MHz, CD$_2$Cl$_2$): δ 155.3, 154.3 (each s, COMe/C$_6$H$_2$(OMe)$_2$), 142.9 (m, Ru−C≡C), 137.9 (m, *ipso*-C$_6$H$_5$ (dppe)), 134.6−134.5 (m, *o*-C$_6$H$_5$ (dppe)), 129.1 (s, *p*-C$_6$H$_5$ (dppe)), 127.3−127.2 (m, *m*-C$_6$H$_5$ (dppe)), 122.9 (s), 115.6 (s), 115.4 (s), 114.7 (s), 105.0 (s), 82.2 (s, C≡CH), 80.7 (s, C≡CH), 56.5 (s, OCH$_3$), 56.4 (s, OCH$_3$), 31.7 (m, |$^1J$(C,P) + $^3J$(C,P)| = 23 Hz, PCH$_2$CH$_2$P). $^{31}$P{$^1$H} NMR (161 MHz, CD$_2$Cl$_2$): δ 53.5 (s, dppe). FT-IR (cm$^{-1}$, ATR) = 3293 (m, ν$_{C≡CH}$), 2102 (w, ν$_{C≡C}$), 2052 (s, ν$_{C≡CRu}$).

***trans*-{Ru(dppe)$_2$}{(μ-C≡C-1,4-C$_6$H$_4$−CH=CH){RuCl(CO)(P$^i$Pr$_3$)$_2$}}$_2$ (4a).** CH$_2$Cl$_2$ (15 mL) was slowly added to a mixture of Ru(dppe)$_2$(C≡C-1,4-C$_6$H$_4$−C≡CH)$_2$ (**3a**, 45.1 mg, 39.3 μmol) and RuClH(CO)(P$^i$Pr$_3$)$_2$ (38.2 mg, 78.6 μmol). After the red solution was stirred for 30 min, the solvent was removed under reduced pressure. The crude product was purified by precipitation by treating a solution of the product in 5 mL of CH$_2$Cl$_2$ with 30 mL of *n*-hexane and stirring for 10 min. After the precipitate was washed with 5 mL of hexane twice and dried in vacuum, the product was obtained as a rose-colored solid. Yield: 79.1 mg (95%). $^1$H NMR (CD$_2$Cl$_2$, 400 MHz): δ 8.43 (d, $^3J$(H,H) = 13.2 Hz, 2H, RuCH=CH), 7.60−7.52 (m, 16H, *o*-C$_6$H$_5$ (dppe)), 7.27−7.19 (m, 8H, *p*-C$_6$H$_5$ (dppe)), 7.08−6.98 (m, 16H, *m*-C$_6$H$_5$ (dppe)), 6.87 (d, $^3J$(H,H) = 7.9 Hz, 4H, *m*-H/Ru−C≡C−C$_6$H$_4$−), 6.67 (d, $^3J$(H,H) = 7.9 Hz, 4H, *o*-H/Ru−C≡C−C$_6$H$_4$−), 5.98 (d, $^3J$(H,H) = 13.2 Hz, 2H, RuHC=CH), 2.88−2.76 (m, 12H, PCHCH$_3$), 2.66 (s, 8H, PCH$_2$CH$_2$P), 1.42−1.28 (m, 72H, PCHCH$_3$). $^{13}$C{$^1$H} NMR (CD$_2$Cl$_2$, 100 MHz): δ 203.1 (t, $^2J$(C,P) = 13.3 Hz, CO), 147.9 (t, $^2J$(C,P) = 10.5 Hz, RuCH=CH), 137.4 (m, *ipso*-C$_6$H$_5$ (dppe)), 134.5 (m, RuCH=CH), 134.4−134.1 (m, *o*-C$_6$H$_5$ (dppe)), 134.0 (s, *p*-C/Ru−C≡C−C$_6$H$_4$−), 129.9 (s, *o*-C/Ru−C≡C−C$_6$H$_4$−), 128.5 (s, *p*-C$_6$H$_5$ (dppe)), 127.1−126.7 (m, *m*-C$_6$H$_5$ (dppe)), 126.7−126.2 (m, *ipso*-C/Ru−C≡C−C$_6$H$_4$−), 123.2 (s, *m*-C/Ru−C≡C−C$_6$H$_4$−), 116.6 (s, Ru−C≡C), 31.4 (m,|$^1J$(P,C) + $^3J$(P,C)|= 23 Hz, PCH$_2$CH$_2$P), 24.4 (vt, *J*(C,P) = 9.7 Hz, PCHCH$_3$), 19.7 and 19.5 (both s, PCHCH$_3$) ppm; the signals for RuC≡C were not observed. $^{31}$P{$^1$H} NMR (CD$_2$Cl$_2$, 100 MHz): δ 54.1 (s, dppe), 39.2 (s, P$^i$Pr$_3$) ppm. HR-MS EI (*m*/*z*): 2120.5584 ([M$^+$], calcd: 2120.55749), 1060.2742 ([M$^{2+}$], calcd: 1060.2782). FT-IR (cm$^{-1}$, ATR) = 2058 (m, ν$_{C≡C}$), 1910 (s, ν$_{CO}$). Anal. Calcd for C$_{110}$H$_{144}$Cl$_2$O$_2$P$_8$Ru$_3$: C, 62.31; H, 6.85. Found: C, 62.20; H, 6.95.

***trans*-{Ru(dppe)$_2$}{(μ-C≡C-1,4-C$_6$H$_4$−CH=CH){RuCl($^{13}$CO)(P$^i$Pr$_3$)$_2$}}$_2$ (4a*).** The synthesis of **4a*** followed the procedure given for **4a**. From 34.8 mg of RuClH($^{13}$CO)(P$^i$Pr$_3$)$_2$ (71.4 μmol) and 41.0 mg of Ru(dppe)$_2$(C≡C-1,4-C$_6$H$_4$−C≡CH)$_2$ (35.7 μmol) 69.4 mg of **4a*** was obtained as a rose-colored solid. Yield: 92%. NMR spectroscopic data are identical to those of unlabeled **4a** apart from the strong enhancement of the Ru(CO) signal in $^{13}$C NMR and the appearance of a broad, unresolved signal at δ = 38.5−37.5 ppm for the P$^i$Pr$_3$ ligands in the $^{31}$P NMR spectrum. FT-IR (cm$^{-1}$, ATR) = 2053 (m, ν$_{C≡C}$), 1858 (s, ν$_{CO}$). Anal. Calcd for C$_{108}$$^{13}$C$_2$H$_{144}$Cl$_2$O$_2$P$_8$Ru$_3$: C, 62.35; H, 6.84. Found: C, 62.22; H, 7.10.

***trans*-{Ru(dppe)$_2$}{(μ-C≡C-1,4-C$_6$H$_2$−2,5-(OMe)$_2$−CH=CH-μ)-[RuCl(CO)(P$^i$Pr$_3$)$_2$]}$_2$ (4b).** *trans*-{Ru(dppe)$_2$}{μ-C≡C-1,4-C$_6$H$_2$−2,5-(OMe)$_2$−C≡CH}$_2$ (**3b**, 0.021 g, 0.02 mmol) and RuClH(CO)(P$^i$Pr$_3$)$_2$ (0.016 g, 0.04 mmol) were treated with 10 mL of CH$_2$Cl$_2$ under nitrogen atmosphere. The deep red solution was stirred for 7 h at RT, and volatiles were removed in vacuum afterward. The crude product was purified by precipitation with *n*-hexane. The solid residue was taken up in 1 mL of CH$_2$Cl$_2$, and that solution was treated with 20 mL of *n*-hexane, which precipitated the product. After the precipitate was washed with 5 mL of *n*-hexane twice and dried in vacuum, the product was obtained as a rose-colored solid. Yield: 0.035 g (91%). $^1$H NMR (400 MHz, CD$_2$Cl$_2$): δ 8.30 (d, 2H, $^3J$(H,H) = 12.5 Hz, RuCH=CH), 7.47−7.56 (m, 16H, *o*-C$_6$H$_5$ (dppe)), 7.11 (t, 8H, $^3J$(H,H) = 7.3 Hz, *p*-C$_6$H$_5$ (dppe)), 6.89 (t, 16H, $^3J$(H,H) = 7.5 Hz, *m*-C$_6$H$_5$ (dppe)), 6.61 (s, 2H, C$_6$H$_2$(OMe)$_2$), 6.26 (d, 2H, $^3J$(H,H) = 12.5 Hz, Ru−CH=CH), 5.86 (s, 2H, C$_6$H$_2$(OMe)$_2$), 3.65 (s, 6H, OCH$_3$), 3.56 (s, 6H, OCH$_3$), 2.90−2.73 (m, 20H, PCH$_2$CH$_2$P and PCHCH$_3$), 1.47−1.25 (m, 72H, PCHCH$_3$). $^{13}$C{$^1$H} NMR (100 MHz, CD$_2$Cl$_2$): δ 203.7 (t, $^2J$(C,P) = 13.3 Hz, CO), 155.1 (s, COMe/C$_6$H$_2$(OMe)$_2$), 149.2 (s, RuHC=CH), 147.9 (s, COMe/C$_6$H$_2$(OMe)$_2$), 138.5 m, *ipso*-C$_6$H$_5$ (dppe)), 134.9 (m, *o*-C$_6$H$_5$ (dppe)), 134.3 (s), 129.2 (RuHC=CH), 128.8 (s, *p*-C$_6$H$_5$ (dppe)), 127.3 (s, *m*-C$_6$H$_5$ (dppe)), 124.4 (s), 117.0 (s), 116.2 (s), 113.9 (s), 107.8 (s), 56.8 (s, OCH$_3$), 56.1 (s, OCH$_3$), 31.7 (m, |$^1J$(C,P) + $^3J$(C,P)|= 23 Hz, PCH$_2$CH$_2$P), 24.4 (t, $^1J$(C,P) = 9.6 Hz, PCHCH$_3$), 20.3, 20.11 (both s, PCHCH$_3$), the signal for RuC≡C was not observed. $^{31}$P{$^1$H} NMR (161 MHz, CD$_2$Cl$_2$): δ 54.6 (s, dppe), 38.08 (s, P$^i$Pr$_3$). HR-MS FAB$^+$ (*m*/*z*): 2240.6014 ([M]$^+$, calcd: 2240.5992). FT-IR (cm$^{-1}$, ATR) = 2045 (m, ν$_{C≡C}$), 1903 (s, ν$_{CO}$). Anal. Calcd for C$_{114}$H$_{152}$Cl$_2$O$_6$P$_8$Ru$_3$: C, 61.12; H, 6.84. Found: C, 60.79; H, 6.61.

***trans*-{Ru(dppe)$_2$}{(μ-C≡C-1,4-C$_6$H$_2$−2,5-(OMe)$_2$−CH=CH-μ)-[RuCl($^{13}$CO)(P$^i$Pr$_3$)$_2$]}$_2$ (4b*).** The synthesis of **4b*** followed the procedure given for **4b**. From *trans*-{Ru(dppe)$_2$}{μ-C≡C-1,4-C$_6$H$_2$−2,6-(OMe)$_2$−C≡CH}$_2$ (0.021 g, 0.02 mmol) and RuClH($^{13}$CO)(P$^i$Pr$_3$)$_2$ (0.017 g, 0.04 mmol) 0.033 g (89%) of **4b*** was obtained. NMR spectroscopic data are identical to those of unlabeled **4b** apart from the strong enhancement of the Ru(CO) signal in $^{13}$C NMR and the appearance of a doublet signal at δ = 38.0 ppm ($^1J$(C,P) = 13.3 Hz) for the P$^i$Pr$_3$ ligands in the $^{31}$P NMR spectrum. FT-IR (cm$^{-1}$, ATR) = 2045 (m, ν$_{C≡C}$), 1858 (s, ν$_{CO}$). Anal. Calcd for C$_{112}$$^{13}$C$_2$H$_{152}$Cl$_2$O$_6$P$_8$Ru$_3$: C, 61.15; H, 6.83. Found: C, 60.76; H, 6.67.


dx.doi.org/10.1021/ic2022177 | *Inorg. Chem.* 2012, 51, 1902−1915

***trans*-{Cl−Ru(dppe)$_2$}$_2$(μ-C≡C-1,4-C$_6$H$_2$−2,5-(OMe)$_2$−C≡C−) ($A_b$).** In a Schlenk tube, [(dppe)$_2$RuCl][OTf] (0.400 g, 0.35 mmol) and HC≡C-1,4-C$_6$H$_2$−2,5-(OMe)$_2$−C≡CH (33 mg, 0.17 mmol) were pumped under vacuum for 30 min. Then, dichloromethane (100 mL) was transferred onto the solids. The solution was stirred during 48 h at room temperature, and then the solution over the formed precipitate was filtered off and the solid rinsed with diethyl ether (2 × 15 mL). Then, dichloromethane (20 mL) commixed with triethylamine (0.30 mL, 3.95 mmol) was saturated with argon and transferred into the Schlenk tube. The mixture was stirred for 15 min and then washed with water (3 × 15 mL) and pentane (3 × 20 mL). The remaining solvent was evaporated to obtain 206 mg of the compound as a poorly soluble yellow solid (59% yield). $^1$H NMR (300 MHz, $CD_2Cl_2$, 297 K): $\delta$ = 7.45−7.08 (m, 80 H, Ph), 5.85 (s, 2 H, C$_6H_2$(OMe)$_2$), 3.51 (s, 6 H, OC$H_3$) 3.02 (m, 8 H, PC$H_2$C$H_2$P), 2.79 (m, 8 H, PC$H_2$C$H_2$P). $^{31}$P NMR (81 MHz, $CD_2Cl_2$, 297 K): $\delta$ = 48.9 (s, P$Ph_2$). FT-IR (cm$^{-1}$, KBr) = 2078 (s, $\nu_{C\equiv CRu}$). HR-MS FAB$^+$ ($m/z$): 2050.3408 ([M$^+$], calcd: 2050.3396). Anal. Calcd for $C_{116}H_{104}O_2Cl_2P_8$.$CH_2Cl_2$: C, 65.79; H, 5.00. Found: C, 66.17; H, 4.88.

**{Ru(P$^i$Pr$_3$)$_2$(CO)Cl}$_2$(μ-CH═CH−1,4-C$_6$H$_2$−2,5-(OMe)$_2$ ($V_b$).** A solution of 1,4-diethynyl-2,5-dimethoxybenzene (0.034 g, 0.19 mmol) in 10 mL of $CH_2Cl_2$ was slowly added to a stirred solution of RuClH(CO)(P$^i$Pr$_3$)$_2$ (0.200 g, 0.41 mmol) in 10 mL of $CH_2Cl_2$. The reaction mixture was stirred for 30 min. The solvent was concentrated under reduced pressure, and the red-colored product was precipitated with addition of MeOH (10 mL). The solvent was filtered off and the product was further washed with MeOH (10 mL) and dried under vacuum. Yield: 0.195 mg (93%). Crystals suitable for structure determination were obtained from recrystallization in chloroform. $^1$H NMR (400 MHz, $CDCl_3$): $\delta$ 8.22 (d, 2H, $^3J$(H,H) = 13.1 Hz, Ru*H*C═CH), 6.54 (s, 2H, C$_6H_2$(OMe)$_2$), 6.21 (dt, 2H, $^3J$(H,H) = 13.2 Hz, $^4J$(H,P) = 2.3 Hz, RuHC═C*H*), 3.64 (s, 6H, OC$H_3$) 2.82−2.69 (m, 12H, PC*H*CH$_3$), 1.38−1.21 (m, 72H, PCHC*H*$_3$). $^{13}$C{$^1$H} NMR (100 MHz, $CDCl_3$): $\delta$ 203.4 (t, $^2J$(P,C) = 13.3 Hz, *C*O), 148.8 (s, *C*OMe/C$_6H_2$(OMe)$_2$), 148.1 (t, $^2J$(C,P) = 10.9 Hz, RuCH═*C*H), 129.0 (t, $^3J$(P,C) = 3.2 Hz, RuHC═*C*H), 125.3 (t, $^4J$(P,C) = 2.2 Hz, *ipso*-*C*/C$_6H_2$(OMe)$_2$), 109.6 (s, *C*H/C$_6H_2$(OMe)$_2$), 56.7 (s, O*C*H$_3$), 24.5 (t, $^1J$(P,C) = 9.9 Hz, P*C*HCH$_3$), 20.1, 20.0 (both s, PCH*C*H$_3$). $^{31}$P{$^1$H} NMR (161 MHz, $CDCl_3$): $\delta$ 37.9 (s, P$^i$Pr$_3$). HR-MS FAB$^+$ ($m/z$): 1158.3723 ([M]$^+$, calcd: 1158.3718). FT-IR (cm$^{-1}$, ATR) = 1899 (s, $\nu_{CO}$). Anal. Calcd for $C_{50}H_{96}Cl_2O_4P_4Ru_2$·MeOH: C, 51.46; H, 8.47. Found: C, 51.22; H, 8.45.

## ■ ASSOCIATED CONTENT

### Ⓢ Supporting Information

X-ray crystallographic data for complexes **2b**, **3b**, $\mathbf{V_a}$ and $\mathbf{V_b}$ in CIF format. Synthetic procedures, spectroscopic and X-ray crystallographic data. This material is available free of charge via the Internet at http://pubs.acs.org.

## ■ AUTHOR INFORMATION

### Corresponding Author

*E-mail: stephane.rigaut@univ-rennes1.fr (S.R.), rainer.winter@uni-konstanz.de (R.F.W.).

## ■ ACKNOWLEDGMENTS

We gratefully acknowledge support of this work by Deutsche Forschungsgemeinschaft (Grant Wi 1272/7-2), the CNRS, the Université de Rennes 1, the ANR (No. ANR-09-JCJC-0025), and the German French intergovernmental S&T cooperation program PROCOPE (DAAD/Egide) .

## ■ DEDICATION

†Dedicated to Prof. Kenneth Caulton on the occasion of his 70th birthday.

## ■ REFERENCES

(1) Astruc, D. *Electron Transfer and Radical Processes in Transition Metal Chemistry*; VCH: New York, 1995.

(2) (a) Demadis, K. D.; Hartshorn, C. M.; Meyer, T. J. *Chem. Rev.* **2001**, *101*, 2655. (b) Chen, P.; Meyer, T. J. *Chem. Rev.* **1998**, *98*, 1439. (c) D'Alessandro, D. M.; Keene, R. F. *Chem. Rev.* **2006**, *106*, 2270. (d) Chisholm, M. H.; Patmore, N. J. *Acc. Chem. Res.* **2007**, *40*, 19. (e) Launay, J.-P. *Chem. Soc. Rev.* **2001**, *30*, 386. (f) D'Alessandro, D. M.; Keene, F. R. *Chem. Soc. Rev.* **2006**, 424. (g) Glover, S. D.; Goeltz, J. C.; Lear, B. J.; Kubiak, C. P. *Coord. Chem. Rev.* **2010**, *254*, 331. (h) Nomura, M.; T. Cauchy, T.; Fourmigué, M. *Coord. Chem. Rev.* **2010**, *254*, 1406. (i) Kaim, W.; Lahiri, G. K. *Angew. Chem., Int. Ed.* **2007**, *46*, 1778. (j) Kaim, W.; Sarkar, B. *Coord. Chem. Rev.* **2007**, *251*, 584. (k) Ward, M. D.; McCleverty, J. A. *Dalton Trans.* **2002**, *3*, 275. (l) Balzani, V.; Juris, A.; Venturi, M.; Campagna, S.; Serroni, S. *Chem. Rev.* **1996**, *96*, 759. (m) Ziessel, R.; Hissler, M.; El-Ghaoury, A.; Harriman, A. *Chem. Soc. Rev.* **1998**, *178−180*, 1251.

(3) (a) Costuas, K.; Rigaut, S. *Dalton Trans.* **2011**, *40*, 5643. (b) Paul, F.; Lapinte, C. *Coord. Chem. Rev.* **1998**, *178−180*, 431. (c) Aguirre-Etchevery, P.; O'Hare, D. *Chem. Rev.* **2010**, *110*, 4839. (d) Low, P. J.; Brown, N. J. *J. Cluster Sci.* **2010**, *21*, 235. (e) Ceccon, A.; Santi, S.; Orian, L.; Bisello, A. *Coord. Chem. Rev.* **2004**, *248*, 683. (f) Záliš, S.; Winter, R. F.; Kaim, W. *Coord. Chem. Rev.* **2010**, *254*, 1383. (g) Rigaut, S.; Touchard, D.; Dixneuf, P. H. *Coord. Chem. Rev.* **2004**, 1586. (h) Ren, T. *Organometallics* **2005**, *24*, 4854. (i) Venkatesan, K.; Blacque, O.; Berke, H. *Dalton Trans* **2007**, 1091. (j) Bruce, M. I.; Low, P. J. *Adv. Organomet. Chem.* **2004**, *50*, 179. (k) Szafert, S.; Gladysz, J. A *Chem. Rev.* **2003**, *103*, 4175. (l) Akita, M.; Koike, T. *Dalton Trans.* **2008**, 3523. (m) Powell, C. E.; Humphrey, M. G. *Coord. Chem. Rev.* **2004**, *248*, 725.

(4) Paul, F.; Costuas, K.; Ledoux, I.; Deveau, S.; Zyss, J.; Halet, J.-F.; Lapinte, C. *Organometallics* **2002**, *21*, 5229. Cifuentes, M. P.; Humphrey, M. G.; Morrall, J. P.; Samoc, M.; Paul, F.; Lapinte, C.; Roisnel, T. *Organometallics* **2005**, *24*, 4280. Samoc, M.; Gauthier, N.; Cifuentes, M. P.; Paul, F.; Lapinte, C.; Humphrey, M. G. *Angew. Chem., Int. Ed.* **2006**, *45*, 7376.

(5) Di Piazza, E.; Norel, L.; Costuas, K.; Bourdolle, A.; Maury, O.; Rigaut, S. *J. Am. Chem. Soc.* **2011**, *133*, 6174. Wong, K. M.-C.; Lam, S. C.-F.; Ko, C.-C.; Zhu, N.; Yam, V. W.-W.; Roué, S.; Lapinte, C.; Fathallah, S.; Costuas, S.; Kahlal, S.; Halet, J.-F. *Inorg. Chem.* **2003**, *42*, 7086.

(6) Qi, H.; Gupta, A.; Noll, B. C.; Snider, G. L.; Lu, Y.; Lent, C.; Fehlner, T. P. *J. Am. Chem. Soc.* **2005**, *127*, 15218.

(7) Liu, Y.; Lagrost, C.; Costuas, K.; Tchouar, N.; Le Bozec, H.; Rigaut, S. *Chem. Commun.* **2008**, 6117. Tanaka, Y.; Ishisaka, T.; Inagaki, A.; Koike, T.; Lapinte, C.; Akita, M. *Chem.—Eur. J.* **2010**, *16*, 4762.

(8) Olivier, C.; Costuas, K.; Choua, S.; Maurel, V; Turek, P.; Saillard, J.-Y.; Touchard, D.; Rigaut, S. *J. Am. Chem. Soc.* **2010**, *132*, 5638. Olivier, C.; Choua, S.; Turek, P.; Touchard, D.; Rigaut, S. *Chem. Commun.* **2007**, 3100. Rigaut, S.; Olivier, C.; Costuas, K.; Choua, S.; Fadhel, O.; Massue, J.; Turek, P.; Saillard, J. Y.; Dixneuf, P. H.; Touchard, D. *J. Am. Chem. Soc.* **2006**, *128*, 5859. Vacher, A.; Benameur, A.; Mback Ndiaye, C.; Touchard, D.; Rigaut, S. *Organometallics* **2009**, *28*, 6096. Rigaut, S.; Massue, J.; Touchard, D.; Fillaut, J.-L.; Golhen, S.; Dixneuf, P. H. *Angew. Chem., Int. Ed.* **2002**, *41*, 4513.

(9) (a) Gauthier, N.; Tchouar, N.; Justaud, F.; Argouarch, G.; Cifuentes, M. P.; Toupet, L.; Touchard, D.; Halet, J.-F.; Rigaut, S.; Humphrey, M. G.; Costuas, K.; Paul, F. *Organometallics* **2009**, *28*, 2253. (b) Powell, C. E.; Cifuentes, M. P.; Morrall, J. P.; Stranger, R.; Humphrey, M. G.; Samoc, M.; Luther-Davies, B.; Heath, G. A. *J. Am. Chem. Soc.* **2003**, *125*, 602. (c) Rigaut, S.; Maury, O.; Touchard, D.; Dixneuf, P. H. *Chem. Commun.* **2001**, 373. (d) Auger, N.; Touchard, D.; Rigaut, S.; Halet, J.-F.; Saillard, J.-Y. *Organometallics* **2003**, *22*, 1638.

(10) (a) Klein, A; Lavastre, O.; Fiedler, J. *Organometallics* **2006**, *25*, 635. (b) Benameur, A.; Brignou, P.; Di Piazza, E.; Hervault, Y.-M.; Norel, L.; Rigaut, S. *New J. Chem.* **2011**, *35*, 2105. (c) Olivier, C.;

Kim, B.-S.; Touchard, D.; Rigaut, S. *Organometallics* **2008**, *27*, 509. (d) Field, L. D.; Magill, A. M.; Shearer, T. K.; Colbran, S. B.; Lee, S. T.; Dalgarno, S. J.; Bhadbhade, M. M. *Organometallics* **2010**, *29*, 957.

(11) Bruce, M. I.; Costuas, K.; Ellis, B. G.; Halet, J.-F.; Low, P. J.; Moubaraki, B.; Murray, K. S.; Ouddai, N.; Perkins, G. J.; Skelton, B. W.; White, A. H. *Organometallics* **2007**, *26*, 3735. Fox, M. A.; Roberts, R. L.; Baines, T. E.; Le Guennic, B.; Halet, J.-F.; Hartl, F.; Yufit, D. S.; Albesa-Jové, D.; Howard, J. A. K.; Low, P. J. *J. Am. Chem. Soc.* **2008**, *130*, 3566. Paul, F.; Ellis, B. G.; Bruce, M. I.; Toupet, L.; Roisnel, T.; Costuas, K.; Halet, J.-F.; Lapinte, C. *Organometallics* **2006**, *25*, 649. Bruce, M. I; Low, P. J.; Costuas, K.; Halet, J.-F.; Best, S. P.; Heath, G. A. *J. Am. Chem. Soc.* **2000**, *122*, 1949. Bruce, M. I.; Elis, B. G.; Low, P. J.; Skelton, B. W.; White, A. H. *Organometallics* **2003**, *22*, 3184. Bruce, M. I.; Costuas, K.; Davin, T.; Halet, J.-F.; Kramarczuk, K. A.; Low, P. J.; Nicholson, B. K.; Perkins, G. J.; Roberts, R. L.; Skelton, B. W.; Smith, M. E.; White, A. H. *Dalton Trans.* **2007**, 5387. Fox, M. A.; Farmer, J. D.; Roberts, R. L.; Humphrey, M. G.; Low, P. J. *Organometallics* **2009**, *28*, 5266.

(12) (a) Mücke, P.; Linseis, M.; Záliš, S.; Winter, R. F. *Inorg. Chim. Acta* **2011**, *374*, 36. (b) Maurer, J.; Linseis, M.; Sarkar, B.; Schwerderski, B.; Niemeyer, M.; Kaim, W.; Záliš, S.; Anson, C.; Zabel, M.; Winter, R. F. *J. Am. Chem. Soc.* **2008**, *130*, 259. (c) Maurer, J.; Sarkar, B.; Záliš, S.; Winter, R. F. *J. Solid State Electrochem.* **2005**, *9*, 738. (d) Maurer, J.; Sarkar, B.; Kaim, W.; Winter, R. F.; Záliš, S. *Chem.—Eur. J.* **2007**, *13*, 10257. (e) Maurer, J.; Sarkar, B.; Schwederski, B.; Kaim, W.; Winter, R. F.; Záliš, S. *Organometallics* **2006**, *25*, 3701. (f) Mücke, P.; Zabel, M.; Edge, R.; Collison, D.; Clément, S.; Záliš, S.; Winter, R. F. *J. Organomet. Chem.* **2011**, *696*, 3186. (g) Man, W. Y.; Xia, J.-L.; Brown, N. J.; Farmer, J. D.; Yufit, D. S.; Howard, J. A. K.; Liu, S. H.; Low, P. J. *Organometallics* **2011**, *30*, 1852.

(13) Zhu, Y.; Clot, O.; Wolf, M. O.; Yap, G. P. A. *J. Am. Chem. Soc.* **1998**, *120*, 1812. Xu, G.-L.; Crutchley, R. J.; DeRosa, M. C.; Pan, Q.-J.; Zhang, H.-X.; Wang, X.; Ren, T. *J. Am. Chem. Soc.* **2005**, *127*, 13354. Rigaut, S.; Costuas, K.; Touchard, D.; Saillard, J.-Y.; Golhen, S.; Dixneuf, P. H. *J. Am. Chem. Soc.* **2004**, *126*, 4072.

(14) Ying, J.-W.; Liu, I. P.-C.; Xi, B.; Song, Y.; Campana, C.; Zuo, J.-L.; Ren, T. *Angew. Chem., Int. Ed.* **2010**, *49*, 954.

(15) Jones, S. C.; Coropceanu, V.; Barlow, S.; Kinnibrugh, T.; Timofeeva, T.; Bredas, J. L.; Marder, S. R. *J. Am. Chem. Soc.* **2004**, *126*, 11782. Albinati, A.; Fabrizi de Biani, F.; Leoni, P.; Marchetti, L.; Pasquali, M.; Rizzato, S.; Zanello, P. *Angew. Chem., Int. Ed.* **2005**, *44*, 5702andreferences therein.

(16) Mahapatro, A. K.; Ying, J.; Ren, T.; Janes, D. B. *Nano Lett.* **2008**, *8*, 2131. Kim, B.-S.; Beebe, J. M.; Olivier, C.; Rigaut, S.; Touchard, D.; Kushmerick, J. G.; Zhu, X.-Y.; Frisbie, C. D. *J. Phys. Chem. C* **2007**, *111*, 7521. Luo, L.; Benameur, A.; Brignou, P.; Choi, S. H.; Rigaut, S.; Frisbie, C. D. *J. Phys. Chem. C.* **2011**, *115*, 19955. Liu, K.; Wang, X.; Wang, F. *ACS Nano* **2008**, *2*, 2315.

(17) Pevny, F.; Di Piazza, E.; Norel, L.; Drescher, M.; Winter, R. F.; Rigaut, S. *Organometallics* **2010**, *29*, 5912.

(18) Lavastre, O.; Even, M.; Dixneuf, P. H.; Pacreau, A.; Vairon, J.-P. *Organometallics* **1996**, *15*, 1530.

(19) Werner, H.; Esteruelas, M. A.; Otto, H. *Organometallics* **1986**, *5*, 2295.

(20) (a) This compound was described in the following reference; however, we propose an alternative synthetic route: see the Supporting Information. (b) Lu, Q.; Liu, K.; Zhang, H.; Du, Z.; Wang, X.; Wang, F. *ACS Nano* **2009**, *3*, 3861.

(21) Touchard, D.; Haquette, P.; Guesmi, S.; Le Pichon, L.; Daridor, A.; Toupet, L.; Dixneuf, P. H. *Organometallics* **1997**, *16*, 3640.

(22) Dirk, S. M.; Price, D. W.; Chanteau, S.; Kosynkin, D. V.; Tour, J. M. *Tetrahedron* **2001**, *57*, 5109.

(23) Atherton, Z.; Faulkner, C. W.; Ingham, S. L.; Kakkar, A. K.; Khan, M. S.; Lewis, J.; Long, N. J.; Raithby, P. R. *J. Organomet. Chem.* **1993**, *462*, 265. McDonagh, A. M.; Whittall, I. R.; Humphrey, M. G.; Hockless, D. C. R.; Skelton, B. W.; White, A. H. *J. Organomet. Chem.* **1996**, *523*, 33. Younus, M.; Long, N. J.; Raithby, P. R.; Lewis, J.; Page, N. A.; White, A. J. P.; Williams, D. J.; Colbert, M. C. B.; Hodge, A. J.; Khan, M. S.; Parker, D. G. *J. Organomet. Chem.* **1999**, *578*, 198. Wong, C.-Y.; Che, C.-M.; Chan, M. C.; W. Han, J.; Leung, K.-H.; Phillips, D. L.; Wong, K.-Y.; Zhu, N. *J. Am. Chem. Soc.* **2005**, *127*, 13997. Koutsantonis, G. A.; Jenkins, G. I.; Schauer, P. A.; Szczepaniak, B.; Skelton, B. W.; Tan, C.; White, A. H. *Organometallics* **2009**, *28*, 2195.

(24) (a) Wu, X. H.; Jin, S.; Liang, J. H.; Li, Z. Y.; Yu, G.-A.; Liu, S. H. *Organometallics* **2009**, *28*, 2450. (b) Wu, X.-H.; Liang, J. H.; Xia, J.-L.; Jin, S.; Yu, G.-A.; Liu, S. H. *Organometallics* **2010**, *29*, 1150. (c) Seetharaman, S. K.; Chung, M.-C.; Englich, U.; Ruhlandt-Senge, K.; Sponsler, M. B. *Inorg. Chem.* **2007**, *46*, 561.

(25) West, P. J.; Schwich, T.; Cifuentes, M. P.; Humphrey, M. G. *J. Organomet. Chem.* **2011**, *696*, 2886.

(26) Babgi, B.; Rigamonti, L.; Cifuentes, M. P.; Corkery, T. C.; Randles, M. D.; Schwich, T.; Petrie, S.; Stranger, R.; Teshome, A.; Asselberghs, I.; Clays, K.; Samoc, M.; Humphrey, M. G. *J. Am. Chem. Soc.* **2009**, *131*, 10293.

(27) Xia, H.; Wen, T. B.; Hu, Q. Y.; Wang, X.; Chen, X.; Shek, L. Y.; Williams, I. D.; Wong, K. S.; Wong, G. K. L.; Jia, G. *Organometallics* **2005**, *24*, 562. Yuan, P.; Wu, X.-h.; Yu, G.-a.; Du, D.; Liu, S. H. *J. Organomet. Chem.* **2007**, *692*, 3588. Wu, X.; Weng, T.; Jin, S.; Liang, J.; Guo, R..; Yu, G.-a.; Liu, S. H. *J. Organomet. Chem.* **2009**, *694*, 1877. Lin, Y.; Yuan, J.; Hu, M.; Yin, J.; Jin, S.; Liu, S. H. *Organometallics* **2009**, *28*, 6402. Li, F.; Cheng, J.; Chai, X.; Jin, S.; Wu, X.; Yu, G.-A.; Liu, S. H.; Chen, G. Z. *Organometallics* **2011**, *30*, 1830.

(28) Hapiot, P.; Kispert, L. D.; Konovalov, V. V.; Saveant, J.-M. *J. Am. Chem. Soc.* **2001**, *123*, 6669.

(29) Marchenko, A. V.; Huffman, J. C.; Valerga, P.; Jiménez Tenorio, M.; Puerta, M. C.; Caulton, K. G. *Inorg. Chem.* **2001**, *40*, 6444.

(30) (a) The presence of several multiple bond stretches upon this first oxidation might be explained with a localized electronic character on the fast IR time scale (see refs 10a, b) or some rotational effects (see ref 30b.). Therefore, concerning the CO stretches, there would be a seeming discrepancy but the electron density differences, if they exist, would be too small to manifest in the CO stretches. However, an important question is whether the number of C≡C stretches is really identical to that of the (electronically) different C≡C moieties, and our previous results cast doubts on this equivalence (see ref 17). Therefore, this point remains speculative. (b) Fox, M. A.; Le Guennic, B.; Roberts, R. L.; Brue, D. A.; Yufit, D. S.; Howard, J. A. K.; Manca, G.; Halet, J.-F.; Hart, F.; Low, P. J. *J. Am. Chem. Soc.* **2011**, *133*, 18433. (c) CostuasK.CadorO.JustaudF.Le StangS.PaulF.MonariA. EvangelistiS.ToupetL.LapinteC.HaletJ.-F.Inorg. Chem.2011

(31) Pichlmaier, M.; Winter, R. F.; Zabel, M.; Záliš, S. *J. Am. Chem. Soc.* **2009**, *131*, 4892.

(32) As an example, tentative deconvolutions of the UV−vis−NIR spectra of complex $\mathbf{4b}^{n+}$ states demonstrate the multitude of transitions within the envelopes. See the Supporting Information.

(33) Rauscher, U.; Bässler, H.; Bradley, D. D. C.; Hennecke, M. *Phys. Rev. B* **1990**, *42*, 9830. Deussen, M.; Bässler, H. *Chem. Phys.* **1992**, *164*, 247.

(34) Kaim, W.; Ernst, S.; Kasack, V. *J. Am. Chem. Soc.* **1990**, *112*, 173. Kasack, V.; Kaim, W.; Binder, H.; Jordanov, J.; Roth, E. *Inorg. Chem.* **1995**, *34*, 1924.

(35) Luo, L. L.; Choi, S. H; Frisbie, C. D. *Chem. Mater.* **2011**, *23*, 631. Choi, S. H.; Kim, B.-S.; Frisbie, C. D. *Science* **2008**, *320*, 1382.

(36) Winter, R. F.; Klinkhammer, K.-W.; Zális, S. *Organometallics* **2001**, *20*, 1317.

(37) Sheldrick, G. M. *SHELXTL-97, Program for Crystal Structure Analysis*; University of Göttingen: Göttingen, Germany, 1997.

(38) Higgins, S. J.; La Pensée, A.; Stuart, C. A.; Charnock, J. M. *Dalton Trans.* **2001**, 902.

(39) Chaudret, B.; Commengues, G.; Poilblanc, R. *Dalton Trans.* **1984**, 1635.


dx.doi.org/10.1021/ic2022177 | *Inorg. Chem.* 2012, 51, 1902−1915